A comparative study performed on two ambient ionization techniques: Desorption Electrospray Ionization Mass Spectrometry (DESI−MS) and Easy Ambient Sonic Spray Ionization Mass Spectrometry (EASI−MS)

Tanam Sanjana Hamid

A thesis submitted to the Faculty of Graduate Studies in Partial Fulfillment of the requirements for the degree of

Master of Science

Graduate Program in Chemistry

York University

Toronto, Ontario

November 2014

Abstract

Main project of my master's thesis involved comparison between two sister methods: desorption electrospray ionization mass spectrometry (DESI−MS) and easy ambient ionization mass spectrometry (EASI−MS). These methods are compared in terms of spatial resolution, limits of detection and imaging capabilities. Their applicability in forensic science was further explored by comparing the MS/MS imaging capabilities. Under the same experimental conditions, we found that both DESI and EASI−MS have similar spray spot size resulting in similar spatial resolution. For the limits of detection (LOD) experiment, the LOD of DESI−MS was found to be lower than EASI−MS by an order of magnitude. When we compared the mass spectra and the chemical images of DESI and EASI, we found that both methods produce similar chemical specificity. When the spectra were carefully inspected, a reduction in signal intensity was observed for EASI−MS compared to DESI−MS demonstrating that the sensitivity of DESI−MS is higher than EASI−MS.

Other projects involved characterization of zebra fish tissue system made up of bile salts, phospholipids and fatty acids. By mapping the spatial distribution of these ions, 2D chemical images of organs such as the stomach, the nervous system and the whole body zebra fish were created. I also studied if matrix can impact ionization of proteins by DESI−MS. The aim was to improve the poor desorption of proteins from the surface of DESI−MS. We concluded that the matrix neither increase nor decreases the ionization efficiency of proteins by DESI−MS.

Acknowledgements

I would like to thank my supervisors Professor Demian R. Ifa and Diethard K. Bohme for giving me the opportunity to become a member of their unique and diverse group. Their guidance has been my strength to keep continuing my studies in chemistry.

I would also like to extend my gratitude to Dr. Elaine Cabral and Dr. Alessandra Tata for their advice and help in the design and planning of my experiments.

The assistance of Alexander Chramow and Dragos Lostun during the execution of my experiments has been very valuable and something I will always be very grateful for.

I would like to thank Farid Ahmed from the Department of Physics and Dr. Voislav Blagojevic for always being there whenever I needed inspiration and motivation.

I would also like to thank my colleagues and friends from the Centre for Research in Mass Spectrometry: Consuelo Perez, Peter Liuni, Gregory K. Koyanagi, Declan Williams, Dr. Stefanie Maedler, Irine Samanithan and Dr. Juslin Lau.

I am grateful to the Department of Chemistry and the Faculty of Graduates Studies.

Table of Contents

List of Tables

List of Figures

Chapter 1

1. Introduction:

1.1 Ambient mass spectrometry

Mass spectrometry is an essential analytical tool in chemistry, biochemistry, pharmacy, medicine and many other related sciences. It is used in structural elucidation of unknown compounds using *m/z* ratio of fragmented ions. . 'Ambient mass spectrometry' allows direct analysis of samples in their native state in an open air environment. This leads to generation of ions and neutrals outside the vacuum system allowing unique experiments to be performed. [2] Conventional mass spectrometry requires many sample pretreatment procedures and involves introduction of the sample into the vacuum environment of mass spectrometer. Therefore, 'Ambient mass spectrometry' has a great prospect in the field of analytical chemistry as it involves analysis of real-life objects such as fingertip imprint, [3] a fruit seed, [4] the surface of a leaf, [5] a freshly cut vegetable slice etc. [6] Due to the above characteristics, more than thirty ambient ionization methods have been developed in last eight years. [7] Among these ambient ionization techniques, most number of publications were in the field of desorption electrospray ionization (DESI) and direct analysis in real time (DART). This makes DESI and DART, the two top ambient ionization techniques. [8]

1.2 Imaging mass spectrometry (IMS)

Imaging mass spectrometry allows visualization of distribution of chemical compounds by creating 2D images. It does so by collecting mass spectra for each spot of the sample. Unlike traditional molecular imaging techniques, 'IMS' does not require labelling. With 'IMS', it is also possible to capture snapshots of small molecules such as lipids that is limited with conventional microscope and electronic microscopic techniques. Therefore, 'IMS' is a major discovery in the field of medical and clinical applications. Ionization technique such as DESI, secondary ion mass spectrometry (SIMS) and matrix−assisted laser desorption/ionization (MALDI) allows 'IMS' experiments to be performed. Unlike MALDI and SIMS, DESI uses ambient pressure for analysis of small molecules in the absence of a crystalline matrix. [49]

1.3 Desorption Electrospray Ionization (DESI)

DESI, an ambient ionization method, was introduced by Cooks and coworkers in 2004. [9] Like many other, ambient ionization methods, DESI follows the ESI (Electrospray Ionization) ion production mechanism. [10] Just like ESI, DESI can convert solution phase analyte into gas phase ions at atmospheric pressure. Main difference between DESI and ESI is that DESI can analyze intact samples without sample preparation step.

In 2006, Eberlin and group introduced desorption sonic spray ionization (DeSSI), [11] later renamed as easy ambient sonic spray ionization (EASI) in 2008. [12] DeSSI can produce gaseous ions at atmospheric pressure without requiring high voltage or heat. DeSSI, therefore, is claimed to be a softer technique than 'ESI' producing ions with low internal energy and low charge state.[13]

1.3.1 Principles of ionization

The primary ionization mechanism in DESI is believed to take place via a 'droplet pick up' mechanism. [2] This process is initiated by wetting the sampling surface with micron sized droplets from sprayed solvent. [14] These micron sized droplets are charged from the use of high voltage. These charged droplets produce a thin liquid film in which the solid phase analyte must dissolve (Fig. 1.1). Further collision of these primary droplets with the surface produces second generation of progeny droplets containing analyte.

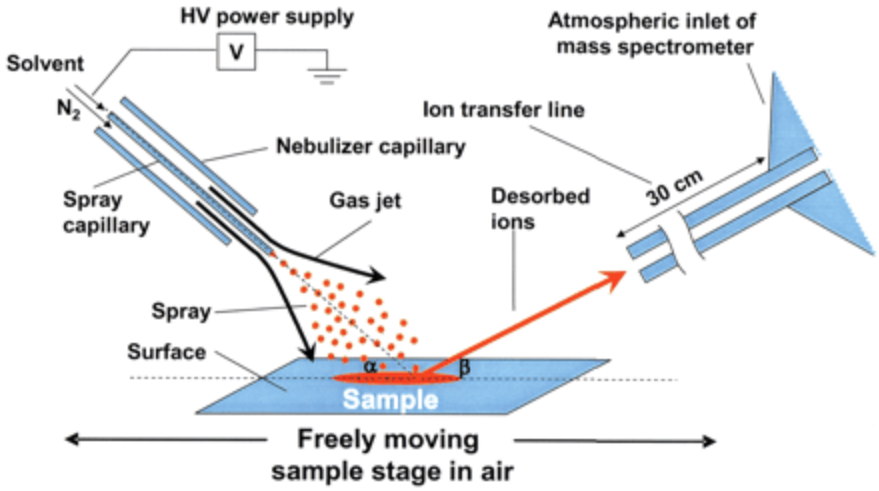

Figure 1.1: Schematic of a typical DESI experiment. The sample solution is dried and deposited on to surface and the solvent is sprayed at a flow rate of typically 1.5 – 10.0 µL/min with application of high voltage (~4 kV). [9]

The analyte acquires charge by a fast charge−transfer reaction with protonated solvent molecule during vaporization to gas phase. [15] The second generation droplets produce an ejection cone travelling downstream towards the mass spectrometer inlet. [16] The average velocity of these droplets is approximately 150 m/s and the average diameter is about 3 μm. [17] According to the ionization mechanism in ESI, application of high voltage (2-5 kV) produces electric gradient between tip of the spraying capillary and inlet of mass spectrometer. This results in charge separation at liquid surface. When 'Coulombic repulsion' at liquid surface is equal to the surface tension of the solution, the solution starts ejecting from the capillary forming a 'taylor cone'. The large droplets projecting outward undergo a series of solvent evaporation and fission events producing smaller droplets which eventually turn into gas phase ions. [18,19]

The median value of the internal energy distribution of ions in DESI is about 2 eV. This value is close to the internal energy distribution of ions produced in ESI. This relatively low internal energy is responsible for minimal fragmentation seen in DESI mass spectra. [20,21] In DESI, nascent ions constantly collide with air particles reducing their average kinetic energy. This is the reason DESI is considered, a soft ionization technique, where low energy intact molecular ions are seen for most compounds.

The schematics of an EASI experiment is similar to the one of DESI (Fig. 1.1), however, the principle ionization mechanism of EASI is based on SSI (Sonic spray ionization). [22] In EASI, nebulizing gas pressure is 2 − 5 times higher than in DESI, [11] producing supersonic gas velocity. This high gas velocity produces positively and negatively charged droplets at atmospheric pressure. The high gas flow rate facilitates the shrinkage of solvent droplet diameter resulting in ions. In this mechanism, the ion intensity is not dependent on voltage/heat/laser. The fast bombardment of atoms with high has velocity produces statistically imbalance distribution of charges resulting in gas phase ions. [23] The mechanism for desorption of analyte from the surface follows the same mechanism as DESI−MS. [16]

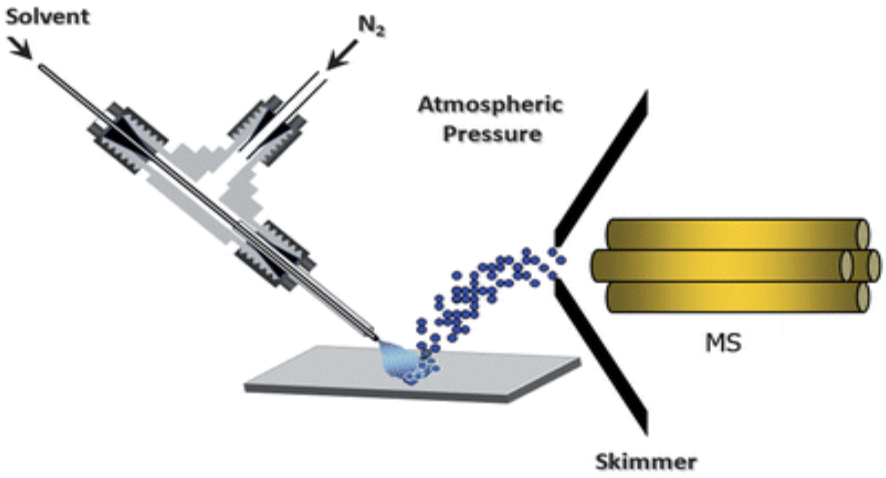

Figure 1.2: Schematic of a typical EASI experiment. Sample solution is sprayed with a typical flow rate of 20−25 µL/min without high voltage or heat. [44]

1.3.2 Instrumentation and Imaging

DESI is a modified version of pneumatically assisted ESI. The micro electrospray source is composed of a sprayer assembly and a surface assembly. Both the spray and the surface can be moved in XYZ position in order to adjust the sprayer to MS or the sprayer to surface distance. High flow nebulizing gas (typically N_2) needs to be supplied from a pressurized source (100-200 psi). Typical solvent flow rate for DESI is in the range of 1.5-10.0 µL/min [1]. It is possible to create two dimensional DESI images by mapping spatial distribution of each analyte that are unique to each species. It is the most useful application of DESI-MS. This is done by capturing the molecular information of the analyte in question and converting it into an optical image

(Fig.1.2). In order to obtain the chemical image, a Thermo-Fisher Scientific LTQ linear ion trap mass spectrometer controlled by Xcalibur 2.0 data processing software is used. This software is

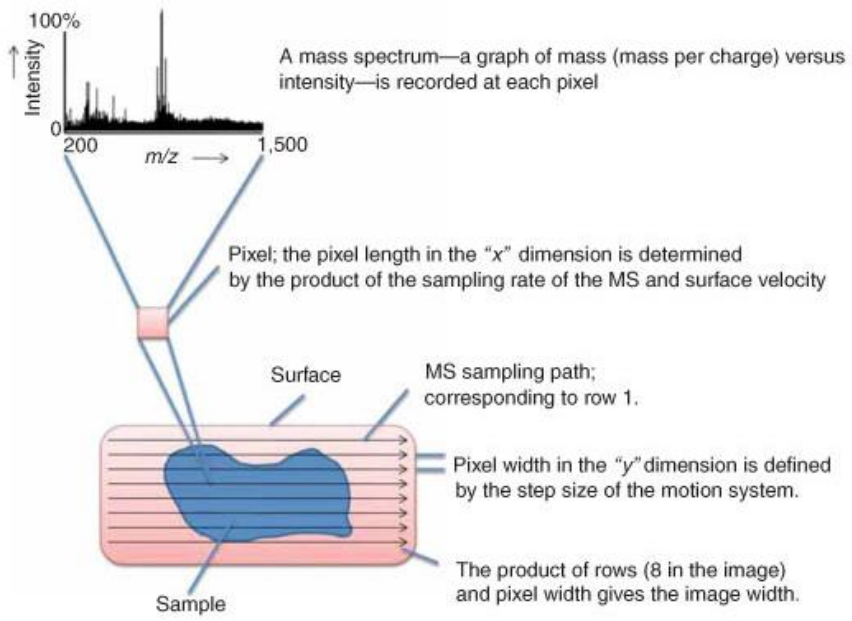

Figure 1.3: Schematic representation of how to convert the mass spectral files into a DESI-MS image [24]

used to create a sample list. The total number of samples in this list must be equal to the total number of lines in the image. An image analysis software known as BioMap (freeware, http://www.maldi-msi.org) is used to process these mass spectral data and transform it into a 2D image of surface vs. intensity. Before visualization of the two-dimensional image, the Xcalibur (.RAW) data files must be converted into BioMap compatible ANALYZE format (.img) through an in-house software known as ImgConverter v3.0. Optimization of DESI sprayer is a must in order to produce a high quality image.

1.3.3 Spatial Resolution

Spatial resolution is defined as the lateral distance between each individual mass measurement determining the pixel size of the resulting image. [49] The most important performance parameter in DESI is the spatial resolution. [25] Typical spatial resolution in DESI is ~ 200 µm, however, under specific conditions; it is possible to achieve a resolution as small as 40 µm. [26] One of the most important applications of DESI-MS experiments is to produce high quality images where smallest features of the image can be distinguished. In order to do so, it is important to obtain the

finest resolution. This resolution is directly correlated to spot size. It is, therefore, absolutely necessary to obtain a spot that is small and well-defined. [7] There are three distinct regions in a sampling spot with most desorption taking place in the inner region. [26] The most effective desorption/ionization area looks like a small elliptical area (Fig. 1.3) where high flow rate for solvent and gas may 'wash' away the analyte without adequate time to be ionized. Careful choice of solvent, surface and flow rate is important to minimize such 'washing effects' and to improve imaging resolution.

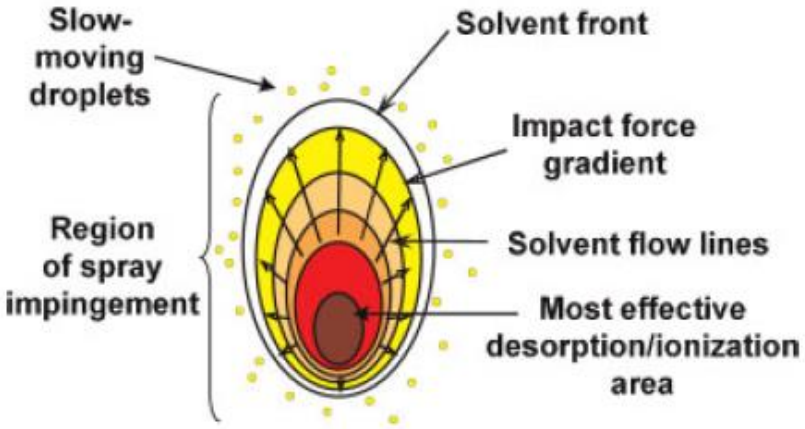

Figure 1.4: Pictorial representation of DESI sampling spot showing the most effective region of ionization [26]

1.3.4 Geometric parameters

There are few ways to control the diameter of these micron sized DESI droplets. One way this can be done is through changing the geometric variables such as the incident angle (α), the collection angle (β), the tip to sampling surface height (d_1), the MS orifice to surface height (d_2) and the sample spot to MS inlet distance (x) (Fig.1.4). An increase in α leads to an increase in signal intensity and a decrease in d_1, leads to an increase in signal strength. Typical values for α are in the range of 45-60° relative to the surface, value of x lies in the range of 2-3 mm, d_1 is typically 1-3 mm and d_2 is usually 1 mm. [1]

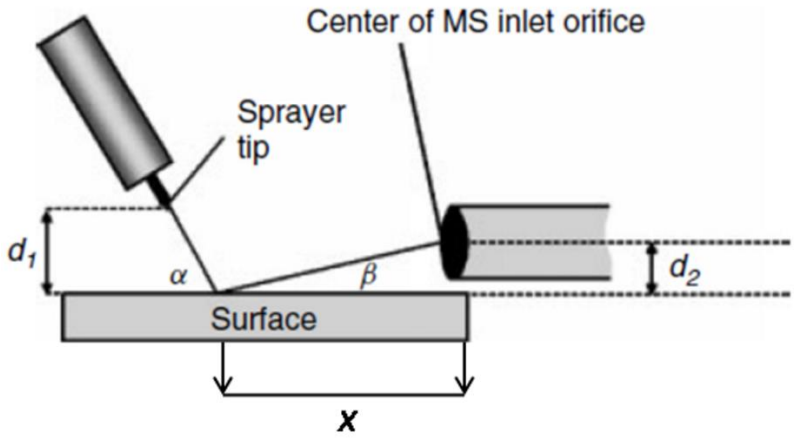

Figure 1.5: Schematic of a DESI-MS set up with the definitions of terms used in DESI [25]

1.3.5 Solvent Effects

The size and shape of the spot in DESI relies heavily on solvent composition. Most common solvents in DESI are composed of 50-70% organic solvents (MeOH, ACN, DMF). [1] It was revealed that the analyte solubility can be increased by changing the aqueous/ organic solvent ratio. Solvents high in organic contents form a better defined elliptical sample spot giving rise to smaller secondary droplets. Smaller droplets are easier to desolvate leading to an increase in ionization efficiency. [27] Moreover, it is possible to control the type of analysis simply by changing the solvent system. For instance, DMF: MeOH or DMF:H_2O make up a better solvent system for solubilizing low molecular weight compounds compare to DMF:ACN or MeOH:H_2O. Solvents rich in organic content can also analyze lipids from the tissue surface without changing the morphology of this in microscopic level. [28]

1.3.6 Surface Effects

Efficiency of DESI also varies a lot depending on the chemical composition, texture and non-insulating properties of the surface. Since in DESI, the particles are already charged when they land, neutralization at the surface must be avoided and therefore, it is preferred to use surfaces that are made up of non-conductive materials. An increased surface affinity may lead to an increase in efficiency of DESI-MS, however, high analyte affinity towards the surface may lead to a loss in sensitivity. This is why DESI surfaces made up of polytetrafluoroethylene (PTFE), polymethylmethacrylate (PMMA) and roughened glass are non conductive and they also

demonstrate limited surface affinity for analytes. [8,25] Signal stability also depends on the polarity of the surface used. For instance, PTFE is a n electropositive polymer and produces strong signals in negative ion mode. PMMA, on the other hand produces stable signals in positive ion mode. [25]

1.4 Applications of DESI-MS

Applications of DESI-MS are wide ranging from forensics to biomedical and pharmaceutical science (Fig.1.5). Lipids play a vital role in biological processes. Distribution of lipid varies depending on the type of tissue. DESI-MS can be applied to map distribution of lipids to characterize tissues such as dog bladder, [29] rat brain [30] and spinal cord, [31] human prostrate, [32] human lens, [33] human atherosclerotic plaques, [34] human kidney, [35] human bladder [36] and human brain, [37] porcine and rabbit adrenal gland. [38] An important application of DESI−MS lipid imaging is the diagnosis of diseases such a tumor. Lipid profiles in biological tissues serve as biomarkers for their diseases. It is possible to map distribution of such lipid profiles through DESI-MS and differentiate between cancerous vs. non-cancerous cells based on several fatty acid or glycerophospholipids (GP) species. [39] Another important application of DESI-MS in the field of biomedical science is to map distribution of small pharmaceutical drugs and their metabolites within animal tissues. For instance, in a study conducted by Cooks and group, rats were orally dosed with clozapine – an antipsychotic drug at 50 mg/kg. [40] The drug and its major metabolites were imaged in rat brain, lung, kidney and testis tissues with DESI-MS. Imaging of metabolites of natural products through imprinting techniques has been another critical application of DESI-MS. Following this technique analytes from soft irregular surfaces can be transferred on to hard, easy to analyze surfaces. Surfaces that have been used to conduct such experiments are cellulose ester filter membrane capturing the exchange of secondary metabolites between bacteria, [41] PTFE and printing paper absorbing metabolites from plant tissues, [42,43] TLC plates capturing metabolites from fruit, vegetable and plan tissues [6] and ordinary printing paper imprinting the metabolites from rat brain tissue and seed. [4] DESI-MS can also be used to create an image of a latent fingerprint by mapping the distribution of an ion of interest. [3] This ion could be from an explosive, drug of abuse, agrochemicals etc. This application has a great prospect in the field of forensic science. Chemical prints of these fingerprints can not only help identify an individual but also help find out about their recent activities.

Similar to DESI−MS, EASI−MS has also been applied in forensic. For instance, in order to identify adulterated inks, [44] fabric softeners [45] and bank notes [46] − EASI−MS, has been found quite useful. In a study to identify counterfeit Brazilian, US and European banknotes, both DESI and EASI−MS were assessed. [46] Using different instruments and experimental conditions, both techniques are able to identify the same number of molecular ions that are used to differentiate counterfeit banknotes. In other reviews, it was suggested to use both techniques side by side to produce strong evidence and rich information for regulated currency monitoring. [8] EASI−MS has also been studied in depth for quality control analysis. For instance, it has been used to check for the purity of biodiesels, fuels and petroleum samples. [47]

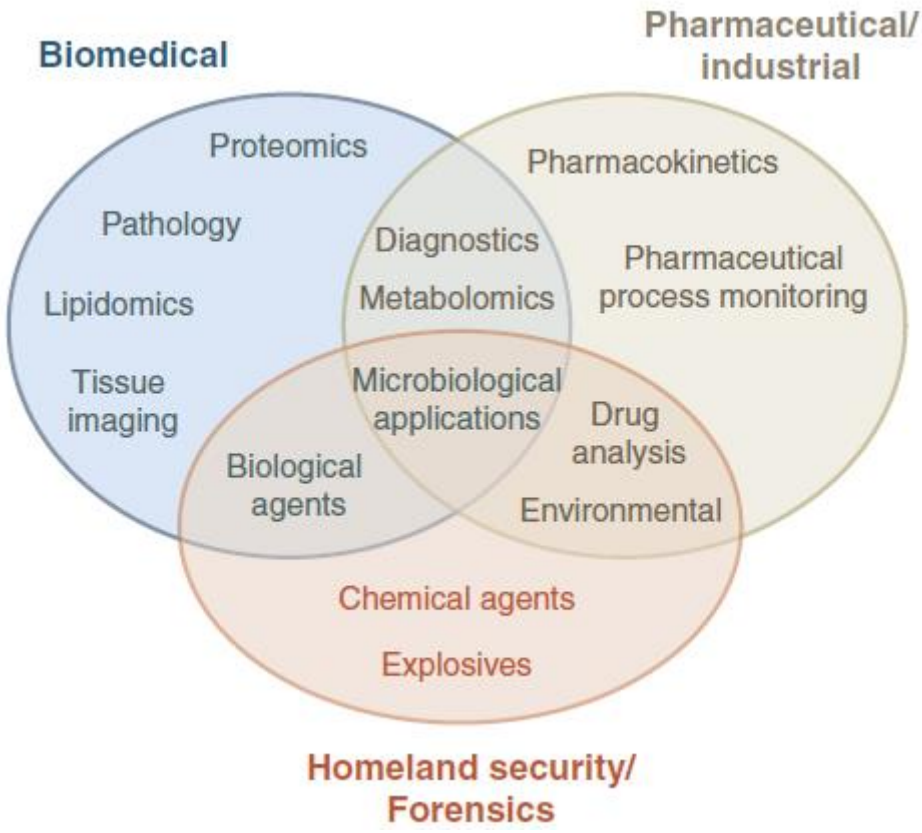

Figure 1.6: Ven diagram demonstrating the areas of application for DESI-MS[48]

For my Master's of Science thesis, I propose to conduct an in-depth study regarding DESI−MS and its applications. I intend to do this by performing a comparative study between EASI (Easy ambient sonic spray ionization) and DESI−MS evaluating the imaging capability of both techniques. This study will evaluate the performance parameters of DESI and EASI−MS in term

of spatial resolution, spot diameter, sensitivity, specificity and limit of detection (Chapter 2). Second chapter my thesis discusses spatial distribution of phospholipids and fatty acids within tissues of stomach, spinal cord and brain of zebra fish (*Danio rerio*), a vertebrate model organism by DESI-MS (Chapter 3). Final chapter (Chapter 4) of my dissertation will discuss the analysis performed on small and large molecular weight proteins. This study is an attempt to improvise ionization of proteins, which otherwise is quite difficult to do by DESI-MS.

Chapter 2

2. Comparisons of ambient spray ionization imaging methods[50]

2.2 Background and Inspiration

In 2012, Norgaard *et al.* published a comparative study between DESI and EASI by producing ion images of tissue sections. [51] The group concluded that EASI can be as efficient as DESI for imaging and direct analysis of tissue sections as long as a higher solvent flow rate (10 µL/min) is maintained. Improved EASI signals were observed when the pressure was kept above 10 bar. The research group found DESI more sensitive than EASI towards analytes that are present at low abundance for both rat brain and plant imprints. This derives the fact that there must be a difference in dynamic range for both DESI and EASI. Norgaard and group did not perform any experiment studying the ionization efficiency and the spray spot size of DESI and EASI. Measurement of spray spot size can determine the size of spatial resolution and spatial resolutions determine image quality. The research paper also does not report any data on quantitative analysis.

2.3 Objective

Our objective is to compare both DESI−MS and EASI−MS in terms of the sensitivity (limits of detection), spray spot size and lateral spatial resolution. We also seek to compare their capabilities on imaging and MS/MS imaging. Detailed research on the experimental conditions of EASI reveal that EASI requires specific conditions such as high gas flow rate (> 3.0 L/min) and high solvent flow rate (> 20 µl/min) to induce ionization of analyte. Such conditions challenge EASI to be categorized as an 'IMS' technique as they destroy biological tissue samples. Therefore, in order to work with all kinds of sample, the experimental conditions of EASI are slightly adjusted by reducing the gas flow rate (< 3.0 L/min) and solvent flow rate (< 10 µl/min). Lower gas flow rate and solvent flow rate will eliminate the signature 'sonic spray' effect of EASI resulting in lower ionization efficiency. In order to accommodate both techniques, we have to work under 'optimized' conditions still allowing the ionization of analyte. Norgaard *et al.* reported that nebulizing gas pressure of 145 psi allows effective ionization and imaging experiments to be performed in EASI without sample destruction. [51] Dewald *et al.* reported that it is possible to perform DESI using a nebulizing gas pressure as high as 170 psi. [52] This is why

we chose the nebulizing gas back pressure to be 140 psi which is still higher than the conventional DESI nebulizing gas pressure but lower than the conventional EASI nebulizing gas pressure (Table 2.1).

In this project, four sets of experiments were performed. First experiment is a spot analysis where solvent spot size is measured on a water sensitive paper under the conditions specified below (Table 2.1). Second experiment evaluated the ionization profiles by analyzing the coronal sections of rat brain. For the third experiment, limits of detections of various compounds on a porous PTFE surface were measured to investigate the ionization and transfer efficiency of both methods. Lastly, MS/MS imaging experiments were performed in order to compare the MS/MS imaging capabilities of DESI and EASI.

Table 2.1. Standard DESI and EASI conditions versus experimental conditions.

	Standard Conditions		Conditions chosen for Limits of detection and Rat brain experiments	
	DESI [53,54]	EASI [55,56]	DESI	EASI
Nebulzing gas back pressure (psi)	50-120	400	140	140
Solvent Flow rate (uL/min)	0.5-5	20-25	1.5/5.0	1.5/5.0
Spray voltage (kV)	2-5	0	5	0

2.4 Experimental

2.4.1 Materials and reagents:

The solvents: methanol, water (HPLC grade) and the compounds used in the limit of detection experiments: propranolol, testosterone, dobutamine, verapamil, chloramphenicol, ibuprofen, diazepam, roxithromycin, and angiotensin, were obtained from Sigma–Aldrich Canada. Porous PTFE sheets 1.5 mm thick with a medium porous size of 7 mm were purchased from Berghof (Eningen, Germany). Microscope slides 26 mm × 77 mm with 1 mm thickness were purchased from Bionuclear diagnostics Inc. (Toronto, ON, Canada). Rat brains were purchased from

(Rockland Immunochemicals Inc., Gilbertsville, PA, USA) and the water sensitive paper was obtained from TeeJet Technologies (Harrisburg, Dillsburg, PA). Red pens containing Rhodamine B and Rhodamine 6G, BIC Company, used in MS/MS experiments were purchased from a bookstore at York University.

2.4.2 Sample preparation

2.4.2.1 Water Sensitive paper: Water sensitive paper was cut to working size of about 5cm by 5 cm and was secured on the moving stage with tape on the all sides.

2.4.2.2 Rat brain: Frozen rat brains were sectioned into 15 µm thick coronal section (12 mm × 15 mm) using a Shandon Cryotome FE (Thermo Fischer Scientific, Nepean, ON, Canada). The cryomicrotome was set at −20 °C while the frozen brain was kept in an insulated box with dry ice. Once the desired temperature was obtained, the rat brain was mounted onto cryotome and the blade was set to slice through the brain at a thickness of 15 µm. These tissue sections were thaw mounted onto glass slides, stored at –18 °C and brought to room temperature before analysis.

2.4.2.3 Limit of Detection: Standards of 1 mg/mL were prepared in methanol. The spotting solutions were created from 1 mg/mL standard using serial dilution to 100, 10, 1, 0.1, and 0.01 ng/µL prepared in a 1:1 ratio of methanol to water solution. Solvent used to spray was also prepared with methanol and water with a ratio of 1:1.

2.4.2.4 MS/MS imaging: Two different red pens were used attempting forgery on a piece of paper. The paper was secured to the running stage with tape and MS imaging was performed.

2.5 Instrumentation

All experiments were carried using an LTQ linear ion trap mass spectrometer (Thermo Fisher Scientific, San Jose, CA, USA) with a lab-built prototype DESI ion source.

2.5.1 Methods

2.5.1.1 Water Sensitive paper: Two tests were performed on water sensitive paper. For the first test, solvent flow rates were varied from 0.5 µL/min to 4.0 µL/min while the nebulizing gas pressure was kept constant at 140 psi. The test also had solvents composed of methanol:water (1:1) and methanol:water (9:1). For the second test, nebulizing gas pressure was varied from 80 psi to140 psi. As the spray solvent, methanol:water (1:1) was applied at a

constant flow rate of 2.0 µL/min. The geometry conditions were set as: spray angle 52°, capillary to inlet distance ~ 3 mm and capillary to surface distance ~ 2 mm. DESI conditions used spray voltage at 5 kV, while EASI used 0 kV, all other parameters were kept the same. In order to ensure the absence of residual charge in the syringe when turning off the voltage and switching from DESI to EASI, a ground wire was connected to the syringe metal tip during EASI experiments. The moving stage was programmed to make five distinct spots; the distance between each spot was 1 mm and the spray was held on each spot for 1 s before moving to the next. This was followed by making a 10 mm long line while moving the spray continuously and slowly at a speed of 200 µm/s. Each line ended with a final spot sprayed for 10 s before moving on to the next line. After the experiment the resulting papers were scanned for visual inspection.

2.5.1.2 Rat brain: EASI experiments were conducted in negative ion mode using a solvent flow rate of 5.0 µL/min of pure methanol and nebulizing gas (N_2) pressure of 140 psi. The scan range for the experiment was 150 to 900 *m/z*, the ion injection time was 120 ms and 3 microscans were averaged for each pixel in the image. Spray angle was set at 52 degrees, the capillary to inlet distance set at ~ 3 mm and capillary to surface set at ~ 2 mm. The experimental conditions for DESI were same as EASI except for the spray voltage at 5.0 kV. While scanning the rat brain, 50 lines of coronal section (half of the brain) were analyzed by EASI and the other 50 lines were analyzed by DESI at a spatial resolution of 150 µm.

2.5.1.3 Limit of Detection (LOD): Shallow parallel indentation lines were drawn on porous PTFE surface. Volumes of 1 mL were pipetted on the line in increasing concentrations of 0.01, 0.1, 1.0, 10, and 100 ng/mL, respectively. The spots were left to dry for about 20 min and analysis was performed by scanning across the line with a speed of 200 µm/s. Optimized geometric parameters for both DESI and EASI are : capillary angle at 52°, capillary to inlet distance set ~ 3 mm and capillary to surface set ~ 2 mm. A solvent flow rate of 1.5 µL/min for methanol:water mixture (1:1, v/v) and a nebulizing gas (N_2) pressure of 140 psi were used. The limits of detection were established by doing MS/MS on the parent ion and monitoring the main daughter ion.

2.5.1.4 MS/MS imaging: Two red pens containing Rhodamine B and Rhodamine 6G were used on a piece of paper. One pen is used to write a ‘3’ and an ‘F’ and the other pen is used to convert the ‘3’ to an ‘8’ and the ‘F’ to a ‘B’. The paper was secured to the moving stage and ion images were obtained. The conditions for both DESI and EASI are: methanol:water (1:1) at a solvent

flow rate of 3.0 µL/min, spray tip to inlet distance 3 mm, and spray tip to surface distance 1 mm. For DESI, spray voltage was 5 kV and nebulizing gas pressure was 100 psi. For EASI, nebulizing gas pressure was 140 psi and spray voltage was 0 kV. Spatial resolution was set at 150 µm, and the Automatic Gain Control (AGC) was turned off. Experiment ran in MS/MS mode (daughter ion scan) was used to monitor 443 *m/z* fragments from 200 to 500 *m/z*, with collision energy of 19 eV.

2.6 Imaging

Ion images were obtained using a lab-built software named ImgCreator that converted the mass spectra files into a format that is compatible with Biomap (freeware, www.msi.maldi.org).

2.7 Results and discussion

Several experiments were performed: (i) the water sensitive paper was used to test the spray impact area; (ii) imaging of rat brain slices was obtained to compare ion images with or without high voltage; (iii) For DESI and EASI, limits of detection for various compounds on porous PTFE were compared and (iv) MS/MS imaging was performed to further evaluate their credentials as an 'IMS' technique.

2.7.1 Water sensitive paper

The water sensitive paper experiment was performed to compare the size of the spray impact spots produced by both DESI and EASI. In Fig. 2.1, the spot areas were produced on water sensitive paper using methanol:water (9:1) and methanol:water (1:1). DESI and EASI lines were alternately created. In Fig. 2.1A the sample spots were sprayed with methanol and water at a ratio of 9:1 and 1:1, and the flow rate was varied from 0.5 µL/min to 4.0 µL/min. In Fig. 2.1B the spray spots were produced from a methanol:water (1:1) solvent mixture at a constant flow rate of 2.0 µL/min and the nebulizing gas (N_2) pressure was varied from 80 to 140 psi.

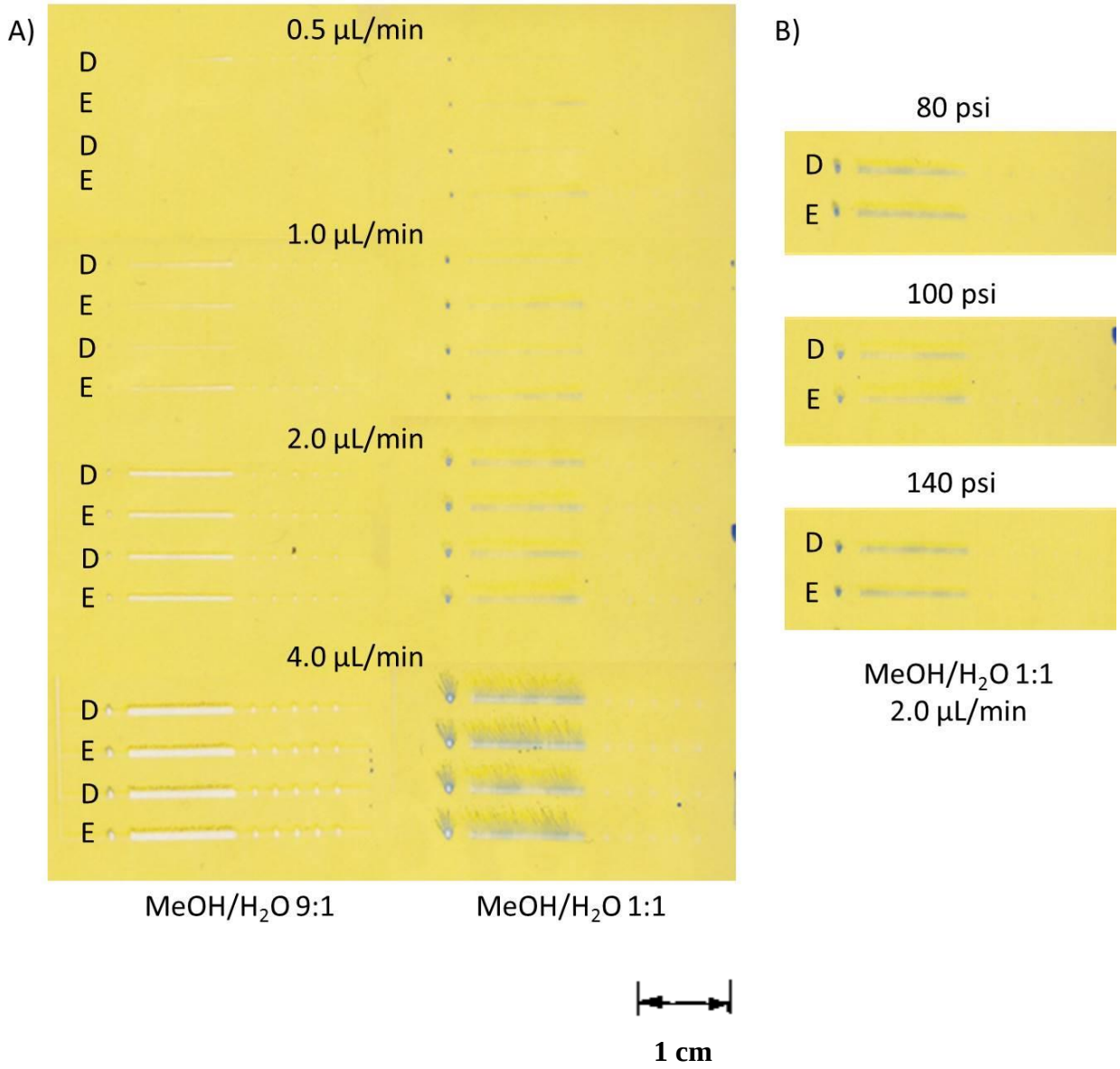

Figure 2.1: Spots and lines produced by DESI−MS (D) and EASI−MS (E) obtained on water sensitive paper using MeOH and H_2O at 9:1 and 1:1 ratio. Column (A) represents spots made with varying solvent flow rates of 0.5 µL/min, 1.0 µL/min, 2.0 µL/min and 4.0 µL/min using both solvent mixtures. Column (B) represents spots made with varying nebulizing gas (N_2) pressure of 80 psi, 100 psi and 140 psi using MeOH and H_2O (1:1) at 2.0 µL/min flow rate.

As the solvent flow rate increases, the spray spot size increases which is evident from Fig. 2.1. Analysis of the spot shape from fig. 2.1 (A) reveals that shape can be controlled by the solvent composition. Methanol evaporates faster than water; as a result, when the concentration of water is higher in the solvent mixture, solvent impact spots tend to smear. Solvent spots in fig. 2.1 (B), made with varying gas pressure, are comparatively similar and almost indistinguishable. This indicates that nebulizing gas pressure does not impact the spray spot size the same way as the solvent composition and the solvent flow rate do. Analysis of the size and shape of the solvent spots obtained for both DESI and EASI reveal that they look similar under various experimental conditions. An absence of high voltage results in a lower number of charged microdroplets without affecting the size of the spot. In the absence of voltage, high gas velocity leads to an unbalanced distribution of charges in the solvent droplets resulting in generation of gaseous ions. This explains why the spray impact spot size should remain the same for DESI and EASI under identical experimental conditions. Since spot size is directly correlated to spatial resolution, similar spot size will also result in similar imaging lateral spatial resolution for both DESI and EASI given the same experimental conditions. Therefore, we can conclude that the major factors contributing to the shape of the spots are the composition of solvents and flow rate, with a small contribution by the gas pressure. If the voltage does contribute to a different spray impact distribution, the effect of the gas seems to make the voltage effect negligible under these operating parameters. Based on these results a low solvent flow rate and medium gas pressure could be used for the imaging of rat brain and the LOD experiments. It is not possible to obtain stable signals by EASI with a flow rate less than 5.0 µL/min. Such high flow rates without smearing effect was only attainable when pure methanol was used as solvent. To ensure efficient ionization for EASI, we chose a gas pressure (140 psi) higher than the typical DESI gas pressure (50 – 120 psi). Anything above 140 psi could not be obtained due to technical limitations.

2.7.2 Rat Brain

Ion images of rat brain (Fig. 2.2) were obtained using both DESI−MS and EASI−MS on the same sample by mapping the spatial distribution of phospholipids which are PE(16:0/22:6) at *m/z* 746.6, PS(16:0/18:1) at *m/z* 760.6, plasmenyl-PE(18:0/22:6) at *m/z* 774.6, PS(18:0/18:1) at *m/z* 788.6, PE(18:0/22:6) at *m/z* 790.6, PS(18:0/22:6) at *m/z* 834.6, sulfolipids that are ST(22:0) at *m/z* 863.0, ST(24:1) at *m/z* 888.7, ST(h24:0) at *m/z* 906.7 and fatty acids which are oleic acid (18:1) at *m/z* 281.5 and arachidonic acid (20:4) at *m/z* 303.4. [57] Structural elucidation of these

ions was obtained through MS/MS experiments. Each kind of phosopholipid/sulfolipid/fatty acid demonstrates signature fragmentation pattern and thus confirming their presence. The mass spectra (Fig. 2.3A and 2.3C) obtained for gray and white matter contain similar ions except for few of them: the white matter contains ions at *m/z* 862.7, *m/z* 888.7 (Fig. 2.3C) while the gray matter does not contain them (Fig. 2.3A). This indicates that the white matter of the brain has various forms of sulfatides (ST) and the gray matter does not have them. The white matter and the gray matter of rat bain also vary in terms of the relative intensities of ions. For instance, the gray matter contains peaks at *m/z* 281.5 and *m/z* 303.5 that have higher intensities compared to the intensities of the corresponding peaks in white matter. When the mass spectra derived by EASI and DESI-MS are compared, both of them appear to contain similar ions (Fig. 2.3A and 2.3C). Therefore, both DESI and EASI have similar chemical specificity, as both techniques can detect the same type of ions. Both techniques displayed stable signals for phospholipids as well as fatty acids. The only difference lies in the absolute intensity of the ions. The absolute intensity for the ions that are present at both high and low abundance seems to be higher for DESI than EASI. In gray matter (Fig. 2.3A), the absolute intensity of the peak at *m/z* 834.6 in DESI spectrum is higher than the absolute intensity of the corresponding peak in EASI spectrum. The higher voltage in DESI-MS is the key to generating a greater number of charged microdroplets containing analyte ions resulting in such higher spectral intensities. Similarly, in white matter (Fig. 2.3C), the absolute intensity of the peak at *m/z* 281.5 in the DESI spectrum is higher than the absolute intensity of the corresponding peak in EASI spectrum. These results also indicate that DESI is a more sensitive technique than EASI as it consistently produces stable signals with higher intensity. Both DESI and EASI demonstrate similar ionization profile. Therefore, it is possible to produce chemical images of rat brains mapping the distribution of all kinds of ions via both techniques. This is evident in fig. 2.2 demonstrating that EASI can be as efficient as DESI for imaging. Apart from the intensity of the ions, both DESI and EASI images also show similar spatial resolution coinciding with our results from the water sensitive paper experiment. This fact, taken together with the data from the water sensitive paper, seems to suggest that not only the spot size but the effective ionization area seem to be similar for both DESI and EASI experimental conditions.

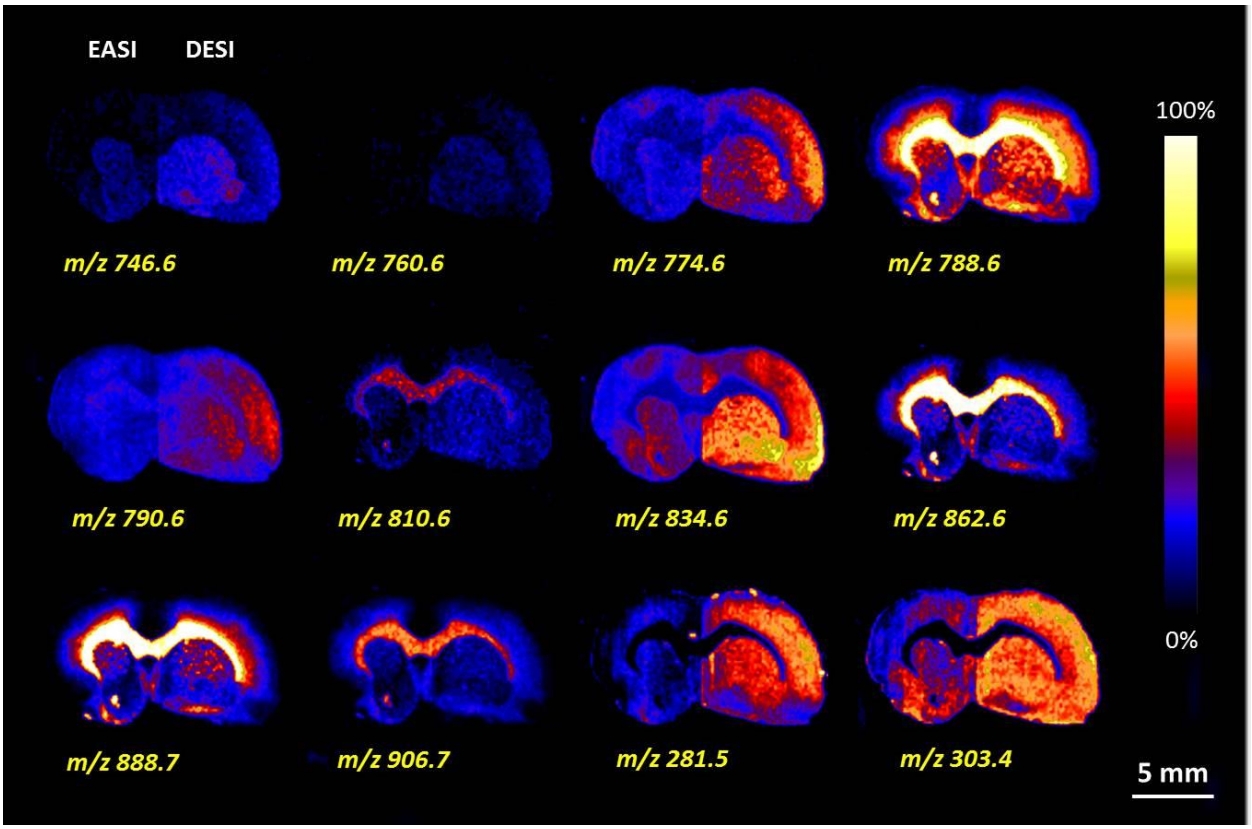

Figure 2.2: Images of selected lipid ions from a 15 µm coronal section of rat brain tissue. Half of the coronal section (50 lines) is scanned by DESI-MS and the other half is scanned by EASI-MS. Both scans are recorded in full scan, negative ion mode. The colour scale bar on the right is an indicator of the ion signal intensity.

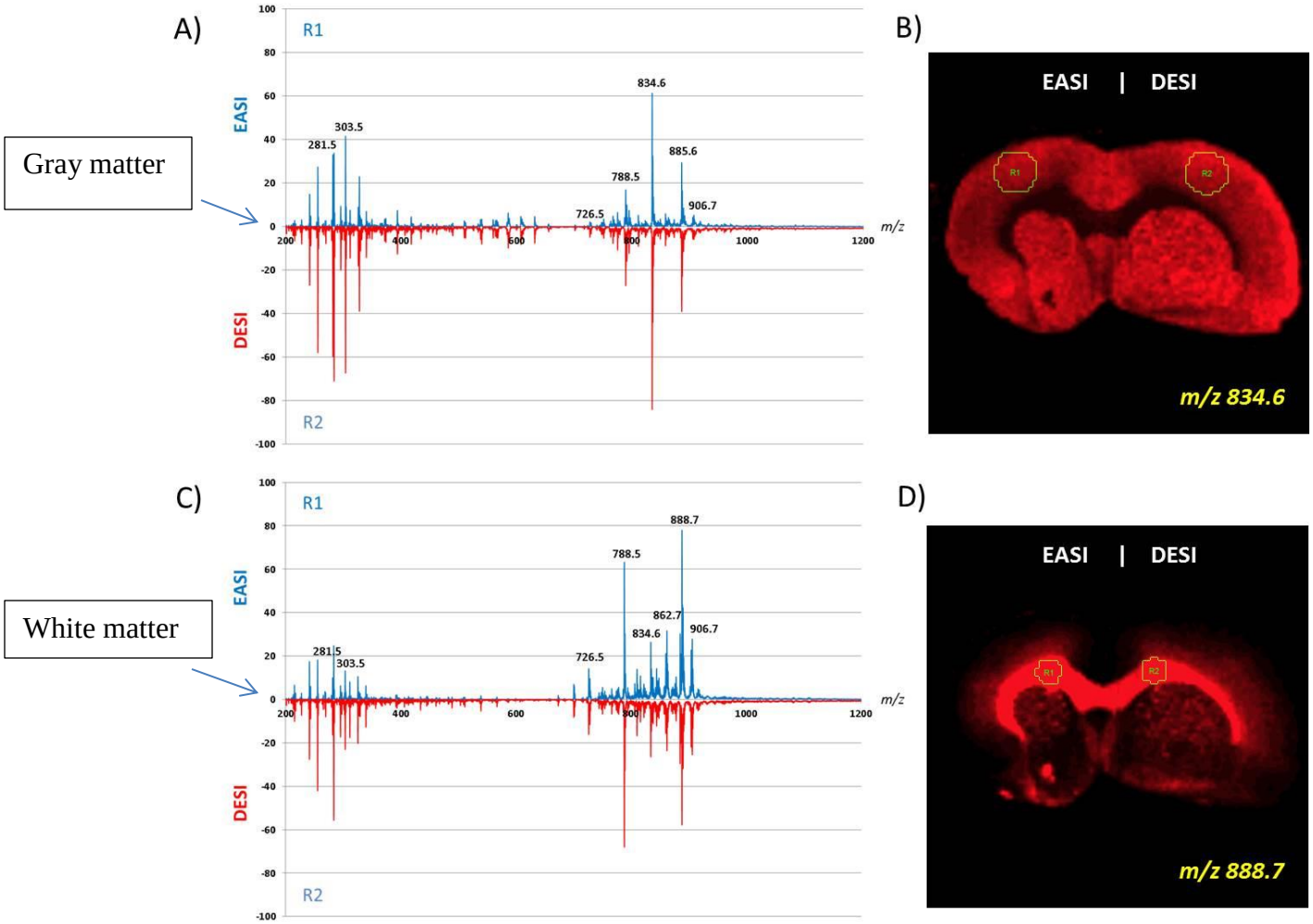

Figure 2.3: The averaged mass spectra (A) obtained through EASI (Top Part) and DESI-MS (Bottom Part) demonstrate distribution of phospholipids and fatty acids at *m/z* 281.5, oleic acid (18:1); *m/z* 303.4, arachidonic acid (20:4); *m/z* 788.5, PS (18:0/18:1); *m/z* 834.6, ST (22:0); *m/z* 885.6, PI(38:4); *m/z* 906.7, ST(H24:0) in gray matter of rat brain. The averaged mass spectra (C) demonstrate distribution of all the phospholipids mentioned above in white matter of rat brain. All four spectra are obtained in negative ion mode. (B) represents the DESI-MS and EASI-MS ion image showing the distribution of ST (22:0). (D) represents the DESI-MS and EASI-MS ion image showing the distribution of PS18:0/18:1).

2.7.3 Limits of detection on Porous PTFE

Limits of detection were investigated on a porous PTFE surface by pipetting the analyte onto the surface in increasing concentrations. This allowed a controlled and reproducible method for determining the lowest concentration detectable under both DESI and EASI parameters. The porous PTFE surface is highly non-polar; this was both a benefit and a challenge. An advantage of using this surface is its ability to concentrate a polar sample onto a small area. A polar solvent, such as water, tends to slide off the surface and not adhere to the surface. Mixing water with methanol improves adherence. Spotting without using guide lines or marks on the surface has led to blank signals along the line. To avoid this issue a shallow line was drawn into surface, this served as both a guide line to ensure all droplets were aligned, but also to facilitate the transfer from the pipette tip to the surface by providing more contact surface between the droplet and the porous material.

The parent ions of the compounds were selected and the daughter ions were monitored across a line in increasing concentrations using selected reaction monitoring (SRM). In SRM mode, ion of a particular mass is selected for the first stage of mass spectrometer and for the second stage of mass spectrometer; fragments of precursor ion are selected and observed. This is how tandem mass spectrometry works. Ions are accelerated by increasing the kinetic energy to the extent where they collide with each other inducing fragmentation. This kinetic energy is known as collision energy (CID). In order to verify the reproducibility of the results, LODs were repeated three times for each compound.

The limits of detection for selected compounds reveal a trend. When voltage is applied, it can decrease the limits by one order of magnitude. Fig. 2.4 is an ion chromatogram obtained for verapamil showing the total ion count for DESI as 3.20E4 and for EASI as 2.85E2. All other compounds were detected at a lower concentration when voltage was applied except for dobutamine and ibuprofen (Table 2.2). The LODs of these two compounds turned out to be the same for DESI and EASI. This deviation of dobutamine and verapamil can be explained by studying proton affinities and solubility of these compounds. Further investigation is necessary to conduct this study.

Table 2.2: Limits of detection of selected compounds using both method conditions on a porous PTFE surface.

Compound	Polarity	Collision Energy (eV)	Precursor → product (*m/z*)	Lowest Conc. Detected (ng/uL) DESI	EASI
Propranolol	+	27	260.2 $[M+H]^+ \rightarrow$ 183.2	0.1	1
Testosterone	+	20	289.3 $[M+H]^+ \rightarrow$ 253.2	10	100
Dobutamine	+	25	302.3 $[M+H]^+ \rightarrow$ 137.2	10	10
Verapamil	+	23	454.4 $[M+H]^+ \rightarrow$ 303.3	0.01	0.1
Chloramphenicol	-	27	321.0 $[M-H]^- \rightarrow$ 257.0	0.01	0.1
Ibuprofen	-	20	205.2 $[M-H]^- \rightarrow$ 161.2	1	1
Diazepam	+	30	285.3 $[M+H]^+ \rightarrow$ 257.1	0.1	1
Roxithromycin	+	20	837.7 $[M+H]^+ \rightarrow$ 679.2	0.01	0.1
Angiotensin	+	20	523.8 $[M+H]^{+2} \rightarrow$ 784.4	1	10

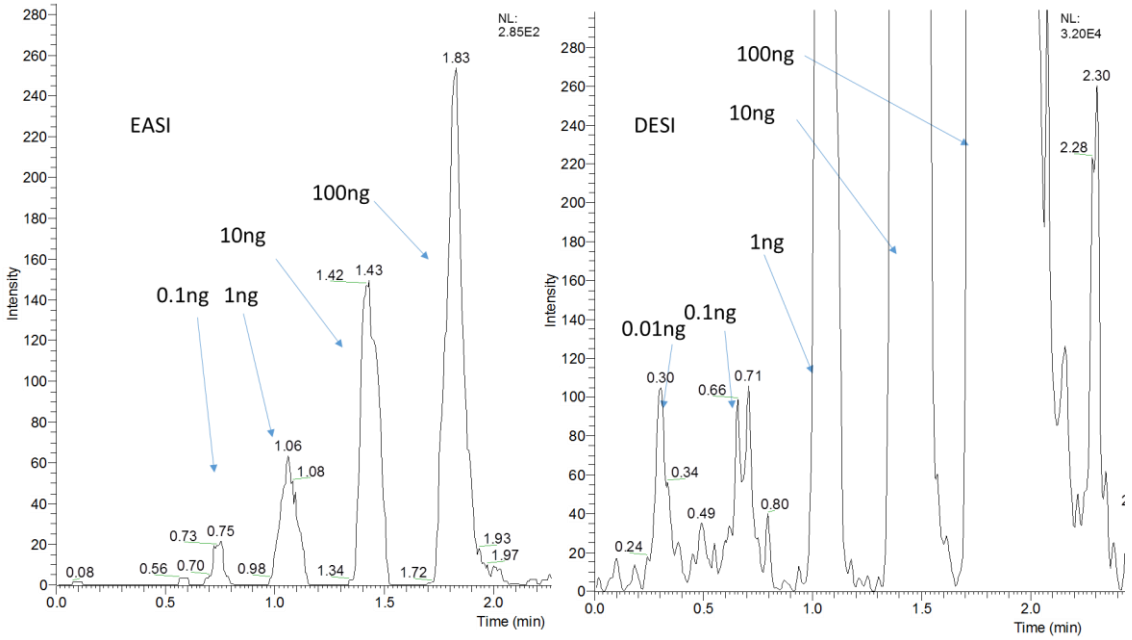

Figure 2.4: Typical scan of a line with spots having concentrations within the range of 0.01 ng to 100 ng/spot. The example above is a scan of Verapamil drug taken with EASI−MS conditions on the left and DESI−MS conditions on the right on an absolute intensities scale versus time.

2.7.4 MS/MS imaging

The capabilities of DESI−MS and EASI−MS to perform MS/MS imaging were compared. This is important in order to distinguish isobaric species and for the analysis of forged documents and other forensic applications. Fig. 2.5 shows an example of the use of red ink where "3 F" handmade characters were converted to "8 B" characters by using a different red ink. Both contain the red ink pigment rhodamine with *m/z* 443 but one is rhodamine B and the other is rhodamine 6G. These two isobaric compounds fragment distinctively. Rhodamine B produces a fragment at *m/z* 399 from a neutral loss of CO_2 and Rhodamine 6G produces a fragment at *m/z* 415 from a neutral loss of ethylene. Fig. 2.5 (e) and (f) illustrate how easy it is to distinguish between the two pens by mapping the fragments and studying the overlap of the fragments. Both DESI and EASI work very well with our particular compound of interest. This is a charged compound so desorption part of the mechanism becomes important. The signal intensity is higher for EASI showing that desorption at higher pressure would outweigh desorption with a charged solvent after a particular point. It is also important to note that use of maximum pressure on a surface greatly depends on the type of sample being used. For instance, biological tissue samples are the hardest to map when the pressure is too high. It may create large droplets with smearing effects producing smudged and low quality images.

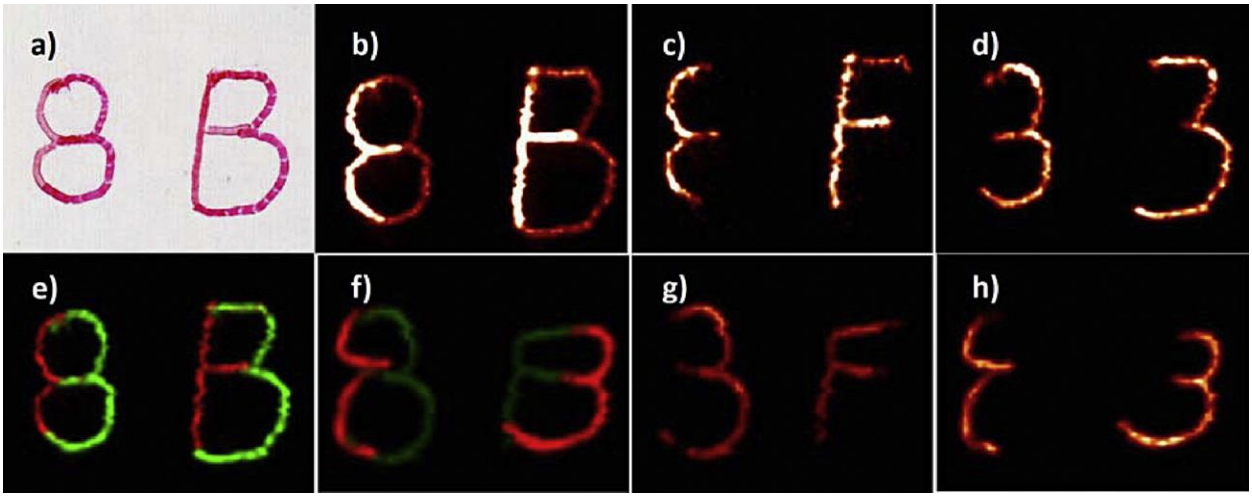

Figure 2.5: (a) Optical image of an 8 and a B made by two different red ink pen formulations to demonstrate an attempt at forging a document, (b) DESI image of the *m/z* 443 ion of the red ink Rhodamine B and Rhodamine 6G, (c) DESI MS/MS image of the

daughter ion *m/z* 399 of Rhodamine B *m/z* 443, (d) DESI MS/MS image of the daughter ion *m/z* 415 of Rhodamine 6G *m/z* 443, (e) DESI MS/MS image of the daughter ion *m/z* 399, in red, of Rhodamine B *m/z* 443 ion and an overlap of the daughter ion *m/z* 415, in green, of Rhodamine 6G *m/z* 443, (f) EASI image of the overlap between ion m/z 399 in green and ion *m/z* 415 in red, (g) EASI MS/MS image of the daughter ion *m/z* 399 of Rhodamine B *m/z* 443, and (h) EASI MS/MS image of the daughter ion *m/z* 415 of Rhodamine 6G *m/z* 443.

2.8 Conclusion

New experiments were performed in order to compare the capabilities of DESI and EASI further and interrogate the viability of EASI as an 'IMS' technique. The water sensitive paper demonstrated minimal difference in spray spot size onto a sample with or without spray voltage indicating that both techniques have similar solvent spray distribution. The spatial resolution for both techniques is similar, thus we can also conclude that EASI has a similar area of ionization as DESI. The voltage has virtually no impact on the solvent spray cone distribution, while it may result in different solvent particle sizes, it does not affect the overall impact area of analyte ionization/desorption. Both methods, under high flow rate conditions, showed signs of smearing the surface. Therefore, solvents with high volatile composition and low flow rates are desired for imaging purposes. The water sensitive paper experiments also revealed that increasing pressure can reduce droplet spread, but not to a significant degree. In imaging experiments high flow rate is undesirable, because it leads to smearing and a larger spray spot area, resulting in low quality images with ambiguous ion distribution. EASI had comparable results with DESI even with a low flow rate illustrating that it has the potential to be used as an 'IMS' technique.

In the limits of detection experiment with no voltage (EASI), the LOD was in some cases the same or an order of magnitude more than DESI. Similar situation was observed for the scan of lipids in the brain tissue. The number of ions detected by both methods were the same with a slight drop in overall signal intensity when no voltage was applied (EASI). While the ion count is lower in EASI than DESI, both techniques result in similar spatial resolution. Both methods can be used for imaging and MS/MS imaging as they both have similar chemical specificity. More investigation is necessary to explain the difference in sensitivity based on physiochemical properties of the analytes and solvents (proton affinity, solubility, pKa, etc.).

Chapter 3

3. Imaging of whole zebra fish (*Danio rerio*) by desorption electrospray ionization mass spectrometry[58]

3. 1 Background and Inspiration

Zebra fish is currently being studied and researched as an ideal vertebrate model organism as it exhibits similar gene sequences and organ systems to humans. [59] Zebra fish has also been used as a model system for studying disease and drug discovery due to their optical clarity. In addition to this, low space requirement, low maintenance cost, rapid generation cycle and rapid development are some of the features making zebra fish ideal for laboratory experiments. [60]

Lipids are diverse molecules in terms of their structure and functionalities and participate in many important cellular processes. [72] Studying lipid composition of various tissue samples can be indicative of their disease state. [61] This is why it is important to characterize biological samples by mapping the distribution of its lipid content as it can be used as a disease diagnostic tool. As building blocks of glycerophospholipids (GP), fatty acids are also important for cellular structure and cellular functions. Lipids and fatty acids are the most common biomolecules found in spinal cord and make up 50% of its dry weight. [73] DESI-MS has been used previously to map distribution of various phospholipids and fatty acids to image rat brain and rat spinal cord [5].

In 2008, Krasowski *et al.* reported that the structure of zebra fish bile salt is composed of four steroid rings and a sulfate functional group. [63] Bile salts are one of the most important biomolecules found in body. Bile salts are mostly synthesized in liver and participate in elimination of cholesterol from liver. They also promote absorption of lipid and lipid soluble vitamins from intestine.

3.2 Objective

Our research goal is to draw a correlation between molecular information and specific tissue system of zebra fish. We intend to broaden the application of DESI-MS in understanding the morphology of species, i.e., zebra fish. In this quest, the above information inspired us to obtain imaging of the intestine, spinal cord and brain of zebra fish by DESI-MS. We planned to do so by mapping the distribution of phospholipids, fatty acids and bile salt.

3.3 Experimental

3.3.1 Materials and reagents

Male adult zebra fish were kindly donated by Dr. Chun Peng's research group (Biology Department, York University). Tricaine mesylate was purchased from Sigma-Aldrich Canada Co. (Oakville, ON, Canada) to euthanize the fish. Carboxymethyl cellulose used to create the moulds was also purchased from Sigma-Aldrich Canada Co. Solvents used were acetonitrile (ACN) (Optima LC/MS) from Fisher Scientific Company (Ottawa, ON, Canada), and N,N-dimethylformamide (DMF) (HPLC grade) from Sigma-Aldrich Canada Co.

3.3.2 Sample preparation

Baby zebra fish was nurtured in a small aquarium with fresh water at room temperature till they reach adulthood. Zebra fish was first euthanized in the aquarium by adding a solution of tricaine mesylate. They were then placed in disposable plastic rectangular frame/ mould (Fig. 3.1) in order to protect them from deformation and damage during cryosectioning. These moulds were filled with carboxymethyl cellulose (CMC) solution and placed immediately in the refrigerator at -20 °C to be chilled overnight. A solution of carboxymethyl cellulose was made by mixing CMC and distilled water until it formed a saturated paste. This embedding medium for zebra fish was carefully chosen according to the work published by Nelson *et al.* [64] This research group reported use of an embedding medium consisting of 5% CMC and 10% gelatin mixture generating reproducible slices of 16 µm thick.

The frozen CMC blocks were removed from the plastic frame and continuously sectioned into 20–60 µm thick sagittal sections at -17 °C using a Shandon cryotome FE and FSE (Thermo Fischer Scientific, Nepean, ON,Canada). The frozen fish slices were thaw mounted on microscope glass slides (Bionuclear diagnostics Inc., Toronto, ON, Canada) (Fig. 3.1) and kept in the freezer at -20 °C until use. The fish slides were then dried in the lab in open air environment for 30 min prior to analysis by DESI-MS.

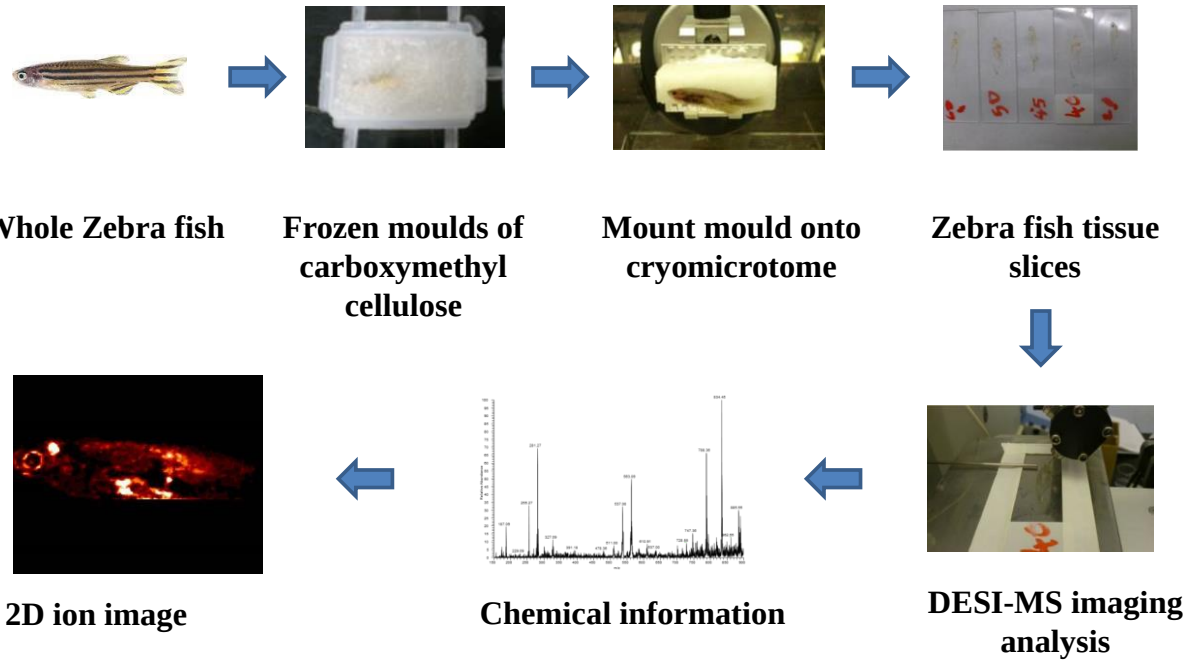

Figure 3.1: Overview of zebra fish tissue processing by DESI-MS

3.4 Instrumentation

All experiments were carried using an LTQ linear ion trap mass spectrometer (Thermo Fisher Scientific, San Jose, CA, USA) coupled to a lab built prototype DESI ion source.

3.4. 1 Methods

The experiment was carried using a morphologically friendly solvent system composed of ACN:DMF (1: 1) at a flow rate of 1.5 µL/min. DESI-MS geometric parameters were chosen as the following: incident angle 52°, spray tip to sampling surface distance ~ 5 mm, distance from the inlet of mass spectrometer to tissue sample ~ 2 mm, collection angle 10°. Experiment was conducted in negative ion mode with spray voltage of 5 kV, injection time of 250 ms, average of 3 microscans and nebulizing gas (N_2) pressure of 100 psi.

3.5 Imaging

LTQ linear ion trap mass spectrometer is controlled by Xcalibur 2.0 software. The zebra fish slice chosen to be imaged has a dimension of 2.5 cm in the x-direction and 0.6 cm in the y-direction. Spatial resolution of the 2D chemical images was selected as 200 µm. The number of lines for the image is determined to be 125 (25000/200) and the number of pixels for each line is determined to be 30 (6000/200). The scan time for each pixel is read as 0.96 s. Therefore, in

order for the whole zebra fish slice to be imaged the total scan time required is approximately 60 min (0.96/scan × 30 scans × 125 lines). The velocity for the surface moving stage turned out to be approximately 208.3 µm/s [(0.96/scan × 30 scans)/3600 s] to acquire mass spectra files within the range of *m/z* 150-900.

Ions of phospholipids, fatty acids and bile salt within mass spectral data are identified from literature. In order to confirm further, MS/MS data were also gathered through collision induced dissociation (CID) tandem MS experiments. CID experiments were performed directly on a tissue slice by moving the sample stage in order to position an area of interest under the spray tip. The CID energy was optimized by manually ramping up the energy from 10–30 units and monitoring the ion fragments. Optimization was attained when a stable signal with multiple ion fragments were produced. The m/z range for the ion selection window was 1.

Once the desired ions are observed and confirmed, an in-house program known as ImgConverter v3.0 was used to convert Xcalibur (.RAW) data files into BioMap compatible ANALYZE format (.img). With Biomap, single ion images of phospholipids as well as fatty acids were obtained. At the same time, images were also created by performing an overlay of two different ion images, i.e. – phospholipids and fatty acids. A rainbow colour gradient was chosen to give the images an interesting colour contrast. Colour intensities for all the ions were also adjusted in a normalized manner so that none of them appears to be more abundant than others.

3.6 Results and discussion

In my thesis, I present the results/scans from a slice that has a thickness of 45 µm. At this thickness, we were able to produce the most reproducible data and observed clear distinction among tissue system belonging to various organs of zebra fish. Once the scan for whole zebra fish slice is done, on BioMap, regions of interest or 'ROI' were selected for the ions we expect to see. We expected to see deprotonated ions of phospholipids and fatty acids in negative ion mode, however, scans were also taken in positive ion mode. Fig. 3.2(a), shows the optical image of 45 µm zebra fish slice which was scanned for the ions of interest. Fig. 3.2(b), is the ion image corresponding to deprotonated oleic acid *m/z* 281. This ion was found to be distributed all over the fish and was previously seen in rat brain as well by DESI-MS. [62] Hence, we decided to use it as a background and compared the images for the rest of the ions against it. Fig. 3.2(c),

demonstrates distribution of phosphatidylserine (PS 40:6) at *m/z* 834. This ion seems to be localized mostly in brain and

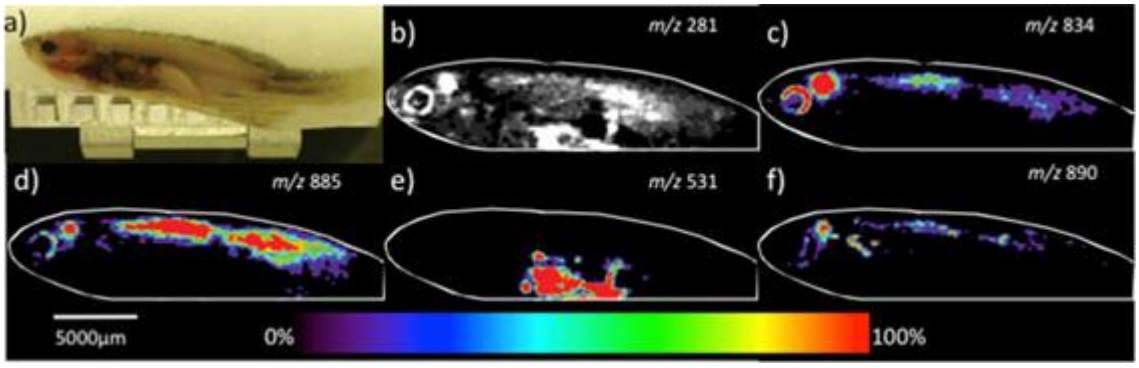

Figure 3.2: (a) Optical image of zebra fish in CMC mould. (b–f) Images of ion distribution produced from DESI analysis. (b) Image of deprotonated oleic acid *m/z* 281, (c) phosphatidylserine (PS 40:6) *m/z* 834, (d) phosphatidylinositol (PI 38:4) *m/z* 885, (e) bile salt 5α-cyprinol 27-sulfate *m/z* 531, and (f) sulfatide (ST 24:0) *m/z* 890.

spinal cord distinguishing these organs from the rest of the zebra fish body. Structural elucidation of this compound is further confirmed by comparing the MS/MS spectrum with literature data (MS/MS: *m/z* 834, 747, 437, 419, 327, 283) (Fig.3.3). [65] The most intense peak at *m/z* 747 $[M - H - 87]^-$ corresponds to the loss of the serine head group (87 Da) confirming the presence of phosphatidylserine within zebra fish brain and spine. The second most intense peak

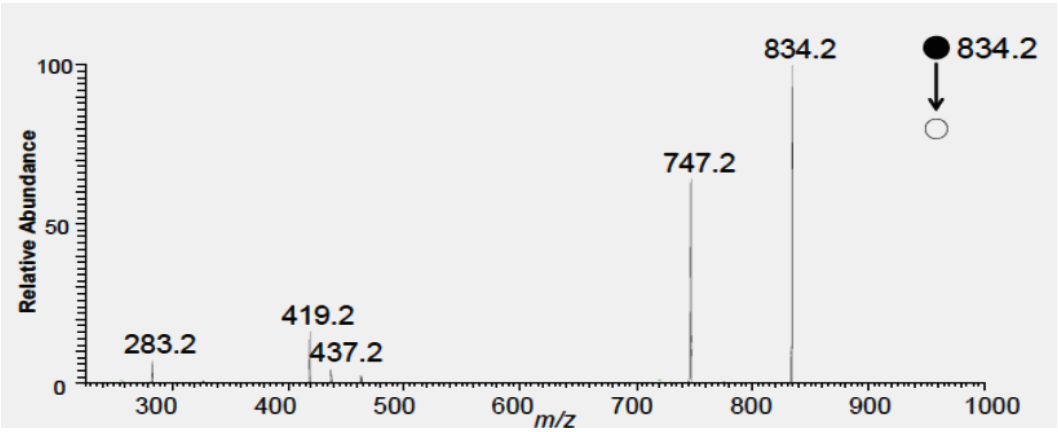

Figure 3.3: MS/MS spectrum of phosphatidylserine at *m/z* 834 [66]

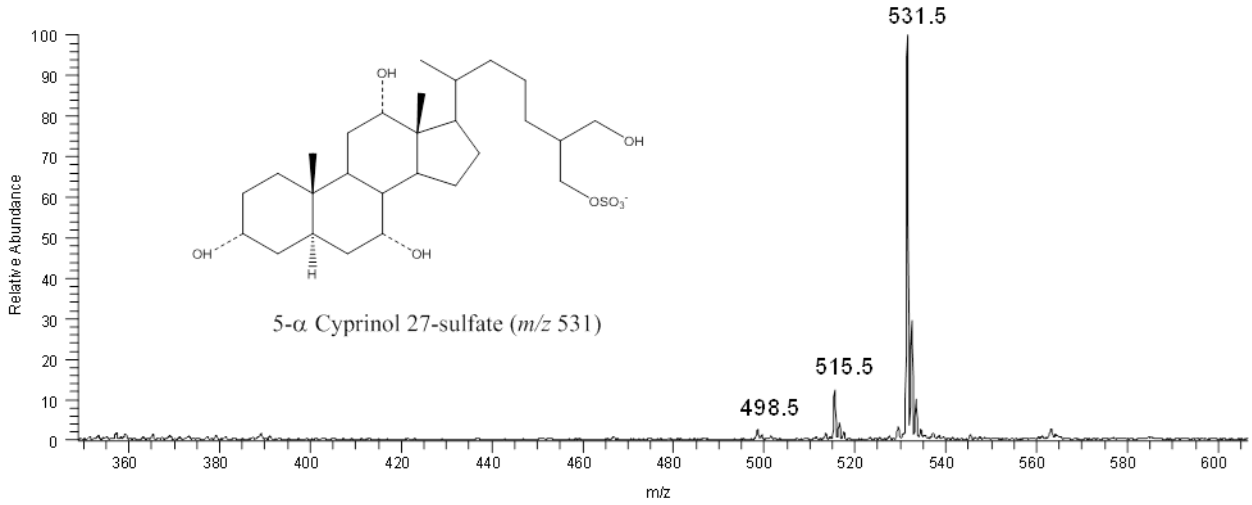

Figure 3.4: DESI−MS of the intestinal system of the zebra fish in negative mode showing: *m/z* 498.5, C24 bile acid-$(OH)_2$-taurine; *m/z* 515.5, C27 bile alcohol-$(OH)_4$-SO_4; and *m/z* 531.5, 5α-cyprinol 27-sulfate.

at *m/z* 419 corresponds to the loss of serine head group and one of the two fatty acid chains. The peak at *m/z* 283 corresponds to the fatty acid anion. [66]

Fig. 3.2(d), illustrates distribution of phosphatidylinositol (PI 38:4) at *m/z* 885 within zebra fish brain and spinal cord. Phosphatidylinositol participates in intracellular communication, [8] therefore, it is expected to be localized and accumulated in neuronal tissue. This assignment was further confirmed by the presence of inositolphosphate (*m/z* 259) in the MS/MS spectrum (MS/MS: *m/z* 885, 599, 581, 419, 303, 283, 259). [67]

Another ion that belongs to the family of phospholipids is mapped in fig. 3.2(f), at *m/z* 890 which is recognized as sulfatide – a sulfolipid. It also bears the fatty acid amide containing ion *m/z* 392 as the fragment was seen in the MS/MS spectrum (MS/MS: *m/z* 890, 872, 652, 522, 392, 258). [67] Sulfatides are present in the myelin sheath and play a very important role in cell differentiation and adhesion. [68] This is why it is not surprising to have found them along the same area of zebra fish brain and spine.

Fig. 3.2(e), represents distribution of bile salts in the form of 5α-cyprinol 27-sulfate at *m/z* 531. The localized area of this ion corresponds to the stomach or intestine of zebra fish. Fig. 3.4 was captured while scanning the intestinal system of zebra fish showing sulfate-conjugated

polyhydroxy bile alcohols at *m/z* 498, 515 and 531. Such signature pattern was previously seen in the work of Krasowski *et al.* [6] who reported that 98% of the bile salts in zebra fish are from 5α-cyprinol 27-sulfate. MS/MS spectrum of bile salts could not be obtained due to signal instability.

3.7 Conclusion

Through our studies performed above, we were able to demonstrate that it is possible to image the different tissue system of zebra fish by DESI-MS. With DESI-MS, we were able to detect and identify ions such as phospholipids and bile salts representing the zebra fish brain, spinal cord and stomach. Therefore, DESI-MS allows characterization of whole zebra fish without extensive sample preparation time. Such direct and quick analysis can allow us to characterize other organisms as well via DESI-MS. The above study can also lead us to research on toxicology, where accumulation of toxins within tissues can be mapped. Fishes are being exposed to harsh conditions such as ionic liquids, detergents and disposals that can have detrimental effects on their very existence. Previous studies conducted on zebra fish have determined the LD_{50} (lethal dose causing 50% death in a population) for various toxins such as metribuzin, [69] xinjunan [70] and endosulfan. [71] Hence, DESI-MS can potentially allow imaging of whole zebra fish via mapping the chemical information derived from toxins and their metabolites.

Chapter 4

4. Producing multiply charged ions of proteins by DESI-MS using matrix

4.1 Background

Proteins are very important biological macromolecules that participate in a wide variety of actions within living organism. Proteins are building blocks of our body participating in almost every cellular process. Analysis of intact protein is extremely important in the field of proteomics. Such analysis can generate information on post-translational modifications of proteins tracking multiple products of a single gene. [74] ESI and MALDI have been the two most popular techniques for the analysis of intact proteins. Both methods require sample pretreatments : dissolving sample molecules in appropriate solvents for ESI and adding solid matrices for MALDI. Another limitation of MALDI is that it can only produce singly charged ion requiring mass spectrometer with a high mass range. On the contrary, DESI-MS is a highly specific technique for high throughout analysis requiring minimal sample treatment. Unlike MALDI, DESI can create multiply charged ions and this is why it has a great prospect for analysis of proteins. [75] The first DESI paper reporting analysis of proteins by Cooks and group came out in 2005. [76] In this paper, proteins like lysozyme, cytochrome c and insulin (MW < 20 kDa) have been analyzed with DESI on surfaces such as glass and PMMA. An absolute detection limit in the range of 10-50 pg has been reported for lysozyme. Through their work, the research group found out that the spectra obtained for DESI−MS are similar to the ones obtained for ESI−MS. However, solvent adduct formation appears to be a common feature during protein analysis in DESI. Cooks and group suggested that this phenomenon can be avoided by changing the instrumental settings such as heated capillary temperature and tube lens voltage. In 2007, Basile and co-workers reported detection of proteins with molecular weight ranging from 12 kDa to 66 kDa [74] by DESI−MS. The research group worked on achieving detection limits for all proteins and found out that the detection limit decreases with decreasing molecular weight. For proteins with a molecular weight ≤ 25 kDa, a signal/noise ratio greater than 5 has been reported. However, for proteins having a molecular weight ≥ 25 kDa, the efficiency of DESI to desorb and ionize protein decreases yielding a signal to noise ratio near or below 3. From these results, it is clear that the analysis of high molecular weight proteins is limited by DESI-MS. In 2013, Venter

and group, investigated the reason for the loss in signal for DESI−MS when high molecular weight proteins are analyzed. [75] The research group studied the two phenomenons: desorption and ionization while they occur independent of each other. From their study, they found out that the larger proteins tend to form solvent or alkali metal adduction as well as dimers or multimers of proteins. Proteins as well as the impurities tend to accumulate in high concentrations when the solvent evaporates This gives rise to additional peaks not resulting from the protonated forms of single protein molecules. Due to the rapid analytic nature of DESI, the droplets are removed too fast to disrupt the protein-contaminant or protein-protein cluster. This is why the application of DESI-MS for the analysis of high molecular weight proteins (> 16 kDa) has been limited.

4.2 Inspiration

In 2012, Inutan *et al.* reported ionization of volatile and nonvolatile compounds with a new ionization method known as 'Matrix Assisted Ionization Vacuum (MAIV)'. [77] In this method, ionization is promoted with the assistance of matrix without requiring high voltage or laser beam or heat. Vacuum at the sample is considered sufficient to induce ionization of analyte. Under such conditions, singly and multiply charged ions of analyte are produced from a surface. As matrix, 3-nitrobenzonitrile (3-NBN) is used that undergoes sublimation/evaporation inducing ionization of analyte. This process is believed to be crucial for generating ions or charged particles. Upon sublimation of matrix and solvation of analyte, charge transfer and particle formation is observed. Using MAIV and the matrix, it is possible to perform sensitive and rapid analysis from various surfaces such as glass, metal and TLC plates. Inutan and group were successfully able to generate negative and positive ions from sample such as drugs, lipids, fatty acids, peptides and proteins using this method. If use of a proper matrix is the key to the analysis of high molecular weight proteins, then the use of high voltage becomes irrelevant. This idea is used as an inspiration for this DESI-MS project.

4.3 Objective

Aim of this experiment is to study the role of matrix in the analysis of proteins by DESI-MS. In this quest, a surface analysis was also performed in order to understand the impact of surface in adsorption and desorption of analyte.

4.4 Experimental

4.4.1 Materials and reagents

Methanol, water and 0.1% formic acid are used to solubilize the analyte. 3-nitrobenzonitrile (3-NBN) is used as matrix. For the analysis of pure proteins, insulin (~5kDa), cytochrome C (~12kDa), lysozyme (~14kDa) and pepsin (~34kDa) are chosen. Solvents (HPLC grade), matrix and pure proteins used in this experiment were purchased from Sigma-Aldrich, Canada. Poly (methyl methacrylate) (Plexiglas) and poly(tetrafluoroehtylene) (Teflon) were purchased from Professional Plastics (Fullerto, CA).

4.4.2 Sample preparation

Pure proteins were diluted with methanol:water (1:1) in order to make a protein standard with a concentration of 10 pmol/µL. Standards of matrix were made by dissolving 5 mg of solid matrix in 5 mL of pure methanol. Matrix:analyte mixture was prepared in a ratio of 1:2 volume ratio, respectively for positive mode analysis. The matrix:analyte spots (Fig. 4.1) were completely dried before DESI−MS analysis.

Figure 4.1: Schematic of matrix:analyte spots made on teflon and plexiglas. Spot 1, 2 and 3 are made with pure proteins. Spot 4, 5 and 6 are made with protein and matrix. Row A corresponds to insulin, row B corresponds to cytochrome c, row C corresponds to lysozyme and row D corresponds to pepsin.

4.4.3 DESI-MS System and Optimization

All experiments were carried using an LTQ linear ion trap mass spectrometer (Thermo Fisher Scientific, San Jose, CA, USA) with a lab built prototype DESI ion source. The electrospray emitter is a Swagelok T-piece composed of two coaxial sections of fused silica capillary tubing. The internal capillary has an inner diameter of 100 μm and an outer diameter of 190 μm. This capillary was connected to the syringe pump through the T-piece spraying solvent. The outer tubing has an inner diameter of 250 μm and an outer diameter of 400 μm and is 15 mm long. Geometric parameters of DESI were set as: spray angle 52 degrees, capillary to inlet distance ~ 3 mm and capillary to surface ~ 2 mm. The spray solvent consisting of methanol:water (1:1) along with 0.1% formic acid was sprayed at 2.0 µL/min. The mass range was set to *m/z* 150-2000 and mass spectra were collected for 1 min in full scan spectral average mode. Measured DESI mass spectra were analyzed using the QualBrowser Xcalibur (ver. 2.1) program.

4.5 Results and discussion

The ability of DESI-MS to identify and detect high molecular weight proteins ranging from 5 kDa to 34 kDa with the aid of matrix was evaluated. Four different proteins with different masses were chosen to perform two different experiments. In one experiment, proteins were analyzed with the aid of matrix (Analysis 1) and the second experiment involved analysis of proteins without matrix (Analysis 2). We expected noise to signal ratio (N/S) to increase with increasing molecular weight of proteins. Two different surfaces (plexiglas and teflon) were tried to evaluate the surface effects on desorption and ionization of proteins. Plexiglas (poly methyl methacrylate) is more hydrophilic than teflon (poly tetrafluoroethylene) by the nature of its chemical constituents. Proteins having plenty of polar residues adsorb better on a hydrophilic surface than on a hydrophobic surface. This is why the N/S for proteins analyzed on teflon turned out to be greater than the N/S for proteins analyzed on plexiglas. Among all proteins analyzed, insulin bears the smallest molecular weight. Therefore, we expected insulin to produce the best quality spectrum. Analysis 2 produced a better quality spectrum (N/S < 5) than analysis 1 (N/S $\leq$ 40) (Fig. 4.2). Among all four spectra, three of them (Fig. 4.2(A), 4.2(B) and 4.3(C)) display peaks showing the charge states +5 (*m/z* 1148), +4 (*m/z* 1434) and +3 (*m/z* 1912) of native insulin. [78]

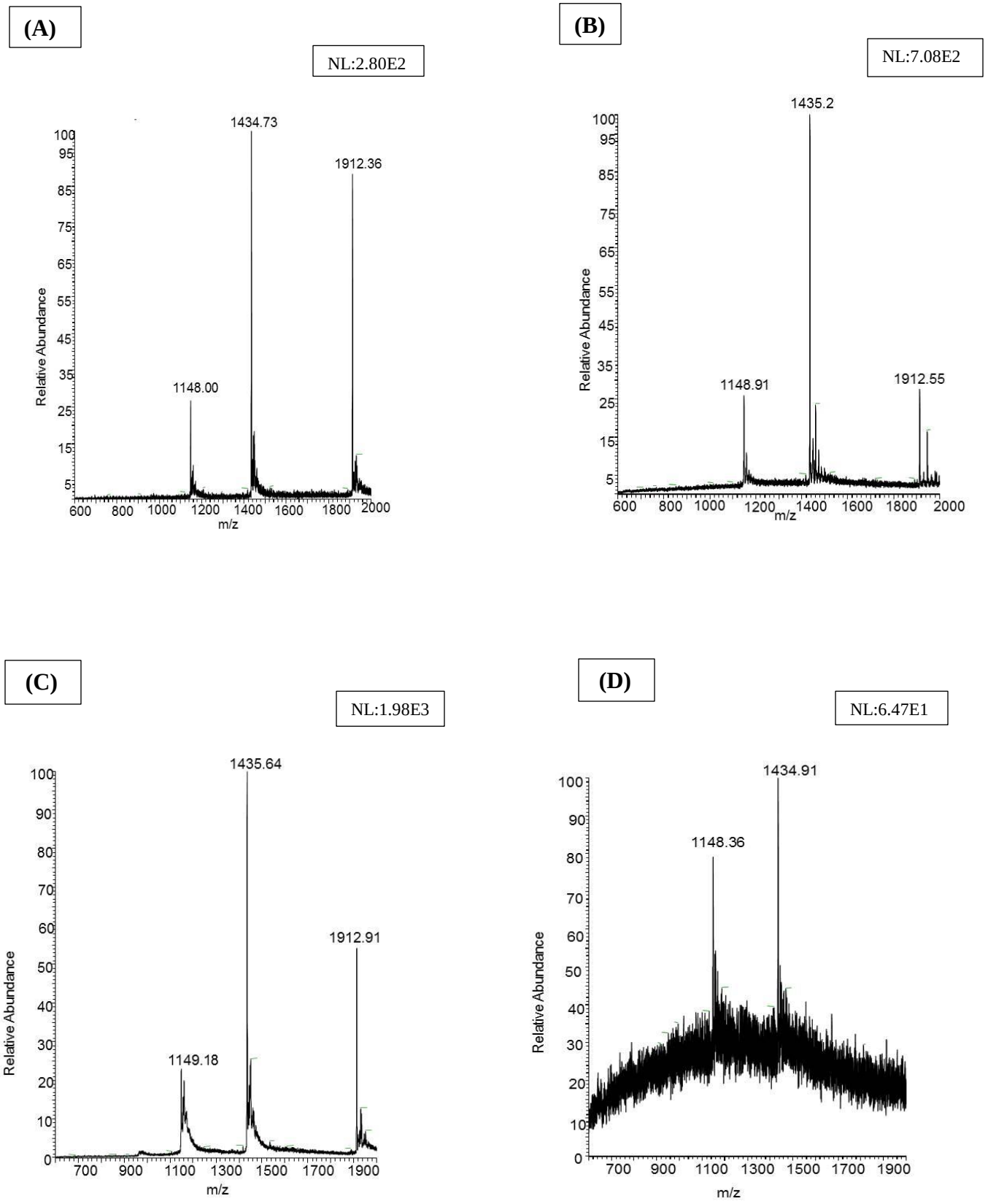

Figure 4.2: Averaged DESI−MS spectrum of insulin on plexiglas (A), insulin on teflon (B), insulin and matrix on plexiglas (C), insulin and matrix on teflon (D).

The spectra above indicate that the analysis done on plexiglas without the application of matrix produced the best quality spectrum for insulin (Fig. 4(A)). The spectrum in fig. 4(A), demonstrates the most stable baseline with N/S < 5. In all four spectra, the peak at *m/z* 1434 demonstrates the highest absolute intensity. When relative intensities are compared, the intensity of the peak at *m/z* 1912 is higher than the intensity of the peak at *m/z* 1148 in fig. 4.2(A) and fig. 4.2(C). In Fig. 4.2(B) the relative intensities at *m/z* 1148 and *m/z* 1912 are comparable and in Fig. 4.2(D), the peak at *m/z* 1912 is missing. This is why the spectra obtained using teflon as the surface are questionable (Fig. 4.2(B) and 4.2(D)). Spectra obtained without matrix on plexiglas also had peak broadening due to a matrix effect. (Fig. 4.2(C)). When fig. 4(A) and fig. 4(C) are compared, the number of peaks detected for insulin remains the same. They only differ from each other in relative intensity of peaks and peak broadening. Therefore, the matrix does not improve the sensitivity for insulin detection by DESI−MS.

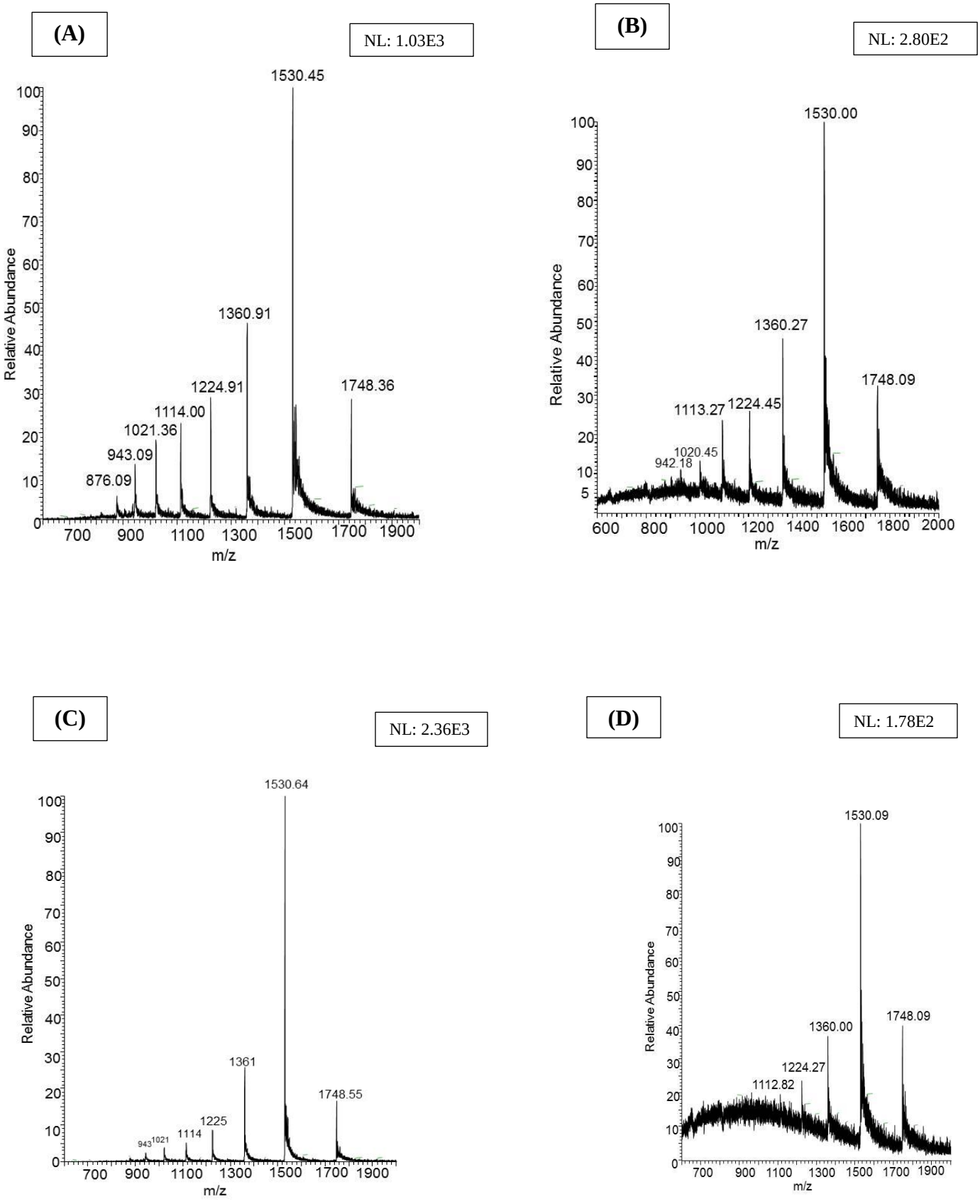

Figure 4.3: Averaged DESI-MS spectrum of cytochrome c on plexiglas (A), cytochrome c on teflon (B), cytochrome c and matrix on plexiglas (C), cytochrome c and matrix on teflon (D).

Spectra obtained for cytochrome c without matrix analyzed on plexiglas display the most number of peaks demonstrating native-type charge state distribution (+7 to +14) consistent with previous work [79] (Fig. 4.3(A)). The spectrum obtained on Teflon for cytochrome c and matrix (Analysis 1), had the most amount of baseline noise (N/S < 20) (Fig. 4.3(D)). In between analysis 1 and analysis 2, analysis 2 produced the most number of ions (Fig. 4.3(A) and 4.3(B)). The absolute intensity of the ion at *m/z* 1530 was the highest in all four spectra. The relative intensity of the ions is comparable in all four spectra. Analysis performed with matrix on plexiglas generated spectra with the most stable baseline and the least amount of peak broadening.

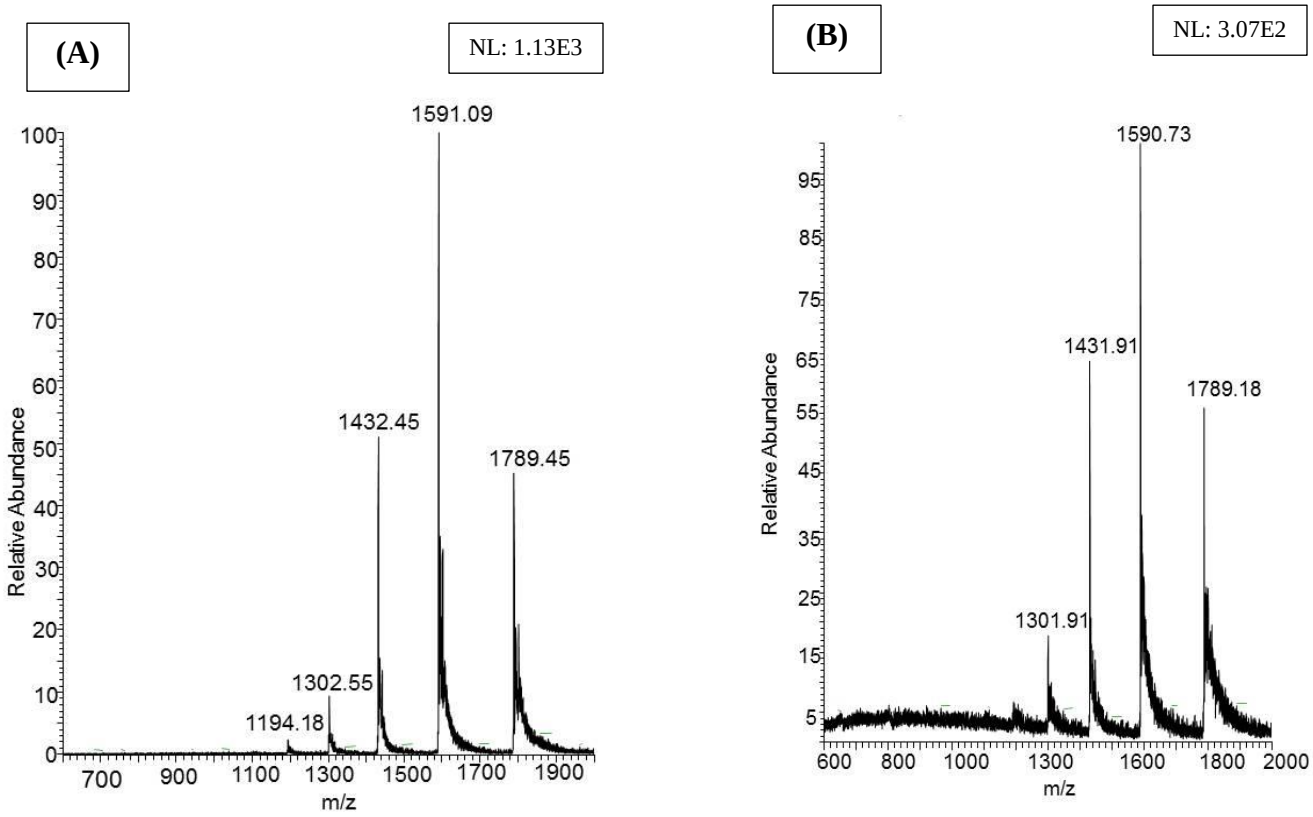

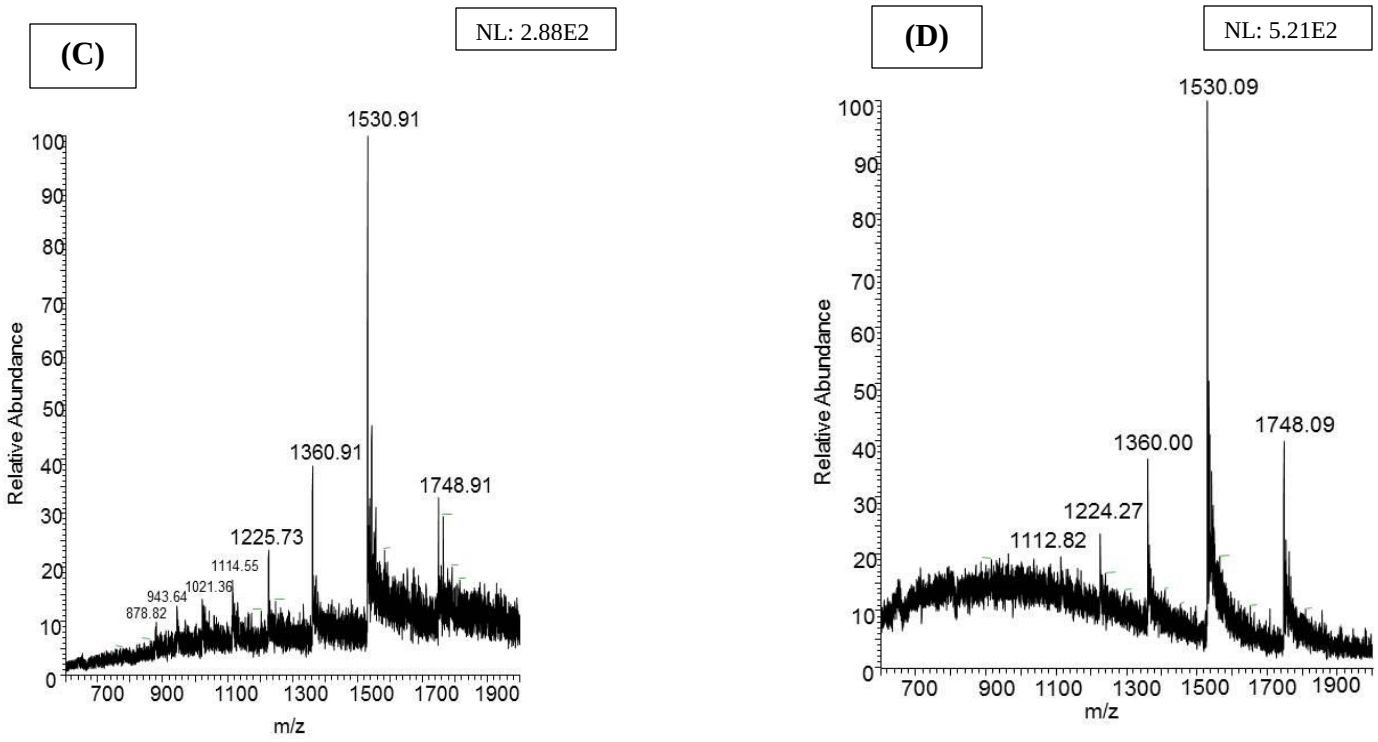

Figure 4.4: Averaged DESI-MS spectrum of lysozyme on plexiglas (A), lysozyme on teflon (B), lysozyme and matrix on plexiglas (C) and lysozyme and matrix on teflon (D).

When all the above four spectra are compared, fig.4.4(A), produces the best quality spectrum with the least amount of baseline noise (N/S < 10) while fig. 4.4(D), produces the worst quality spectrum (N/S < 20). According to the paper by Dasgupta *et al.*, native lysozyme has multiple charged states ranging from +5 to +14. [80] Out of all the above four spectra, fig. 4.4(C), has the most number of ions. These ions are *m/z* 878 with +14 charged state, *m/z* 943 with +13 charged state, *m/z* 1021 with +12 charged state, *m/z* 1114 with +11 charged state, *m/z* 1225 with +10 charged state, *m/z* 1360 with +9 charged state, *m/z* 1530 with +8 charged state, *m/z* 1748 with +7 charged state. The rest of the spectra (fig. 4.4(A), 4.4(B) and 4.4(D)) only generate five peaks. In between analysis 1 and analysis 2, analysis 2 (without application of matrix), produced spectra with the most stable baseline.

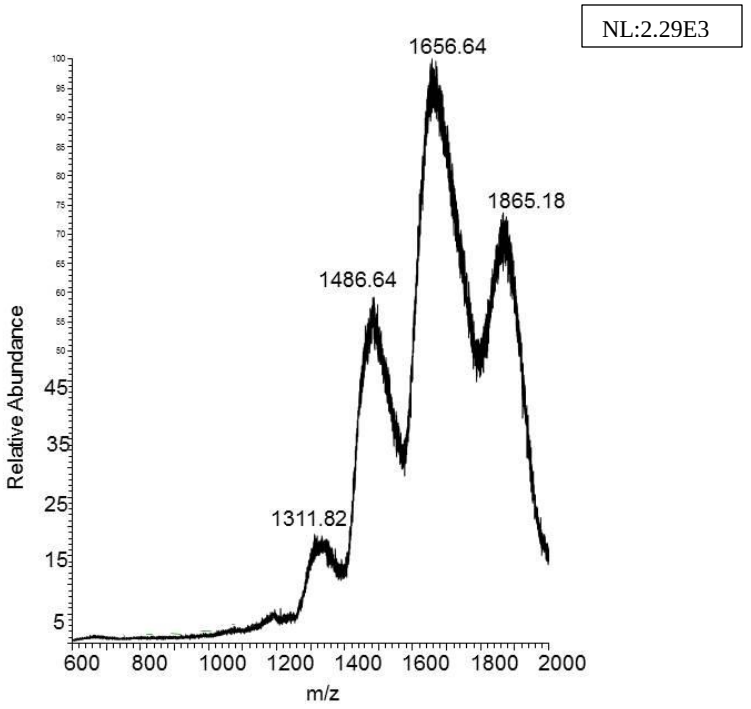

Figure 4.5: Averaged DESI-MS spectrum of pepsin without matrix on plexiglas

Pepsin has the highest molecular weight among all proteins analyzed in this project. This is why it was very difficult to obtain clear and legible data for this protein. The only spectrum achieved was for the analysis on plexiglas without application of matrix (Fig. 4.5). Pepsin is a highly acidic protein making it difficult to generate multiply protonated molecule below m/z 2000. [81] This is why a positive ion mass spectrum is scarce for pepsin. Overall, polycationic species of pepsin are not abundant resulting in insufficient data to produce stable signal.

The above results are a significant find as it clearly explains the role of matrix in the analysis of proteins by DESI-MS. In the paper by Inutan et al., it was proposed that the sublimation of matrix facilitates ionization of analyte without the need of high voltage or laser beam or heat. [77] However, the role of matrix in adsorption and desorption of proteins by DESI-MS is questionable. For almost all four proteins, spectra obtained without matrix demonstrated low

noise to signal ratio. Addition of matrix to the analyte (analysis 1) does not improvise the extraction efficiency of proteins from the surface. A possible explanation of this phenomenon could be rapid removal of analyte from the surface. The process of ionization of DESI-MS requires use of high pressure gas which can speed up the sublimation of matrix without allowing sufficient time for the protein molecule to be picked up along with it. Therefore, the matrix does not contribute towards increasing the ionization and desorption efficiency of proteins.

4.6 Conclusion

The results demonstrated that DESI-MS is a viable approach for analysis of intact proteins that have a molecular weight of $\leq$ 18 kDa. Above a mass of $\geq$ 20 kDa, detection of proteins is poor. This leads to an increasing N/S with an increasing molecular weight of proteins. In order to improve the performance, a matrix solution was chosen that will sublime and ionize proteins creating multiply charged states without the help of high voltage or laser or heat. Through our work, it was found out that the matrix evaporates too fast with the aid of high pressure gas without generating sufficient analyte ions. Hence, the matrix cannot improve ionization of proteins to be detected by DESI-MS.

5. References

1. Monge ME, Harris GA, Dwivedi P, Fernandez FM. Mass spectrometry: Recent advances in direct open air surface sampling/ionization. *Chem Rev (Washington, DC, U S)*. 2013;113(4):2269-2308.

2. Cooks RG, Ouyang Z, Takats Z, Wiseman JM. Detection technologies. ambient mass spectrometry. *Science*. 2006;311(5767):1566-70.

3. Ifa DR, Manicke NE, Dill AL, Cooks RG. Latent fingerprint chemical imaging by mass spectrometry. *Science (Washington, DC, U S)*. 2008;321(5890):805.

4. Ifa DR, Srimany A, Eberlin LS, et al. Tissue imprint imaging by desorption electrospray ionization mass spectrometry. *Anal Methods*. 2011;3(8):1910-1912.

5. Jackson AU, Tata A, Wu C, et al. Direct analysis of stevia leaves for diterpene glycosides by desorption electrospray ionization mass spectrometry. *Analyst (Cambridge, U K)*. 2009;134(5):867-874.

6. Cabral EC, Mirabelli MF, Perez CJ, Ifa DR. Blotting assisted by heating and solvent extraction for DESI-MS imaging. *J Am Soc Mass Spectrom*. 2013;24(6):956-965.

7. Wu C, Dill AL, Eberlin LS, Cooks RG, Ifa DR. Mass spectrometry imaging under ambient conditions. *Mass Spectrom Rev*. 2013;32(3):218-243.

8. Harris GA, Galhena AS, Fernandez FM. Ambient sampling/ionization mass spectrometry: Applications and current trends. *Anal Chem (Washington, DC, U S)*. 2011;83(12):4508-4538.

9. Takats Z, Wiseman JM, Gologan B, Cooks RG. Mass spectrometry sampling under ambient conditions with desorption electrospray ionization. *Science (Washington, DC, U S)*. 2004;306(5695):471-473.

10. Harris GA, Nyadong L, Fernandez FM. Recent developments in ambient ionization techniques for analytical mass spectrometry. *Analyst (Cambridge, U K)*. 2008;133(10):1297-1301.

11. Haddad R, Sparrapan R, Eberlin MN. Desorption sonic spray ionization for (high) voltage-free ambient mass spectrometry. *Rapid Commun Mass Spectrom*. 2006;20(19):2901-2905.

12. Haddad R, Sparrapan R, Kotiaho T, Eberlin MN. Easy ambient sonic-spray ionization-membrane interface mass spectrometry for direct analysis of solution constituents. *Anal Chem*. 2008;80(3):898-903.

13. Takats Z, Wiseman JM, Gologan B, Cooks RG. Electrosonic spray ionization. A gentle technique for generating folded proteins and protein complexes in the gas phase and for studying ion-molecule reactions at atmospheric pressure. *Anal Chem*. 2004;76(14):4050-8.

14. Costa AB, Graham Cooks R. Simulated splashes: Elucidating the mechanism of desorption electrospray ionization mass spectrometry. *Chem Phys Lett*. 2008;464(1-3):1-8.

15. Badu-Tawiah A, Cooks RG. Enhanced ion signals in desorption electrospray ionization using surfactant spray solutions. *J Am Soc Mass Spectrom*. 2010;21(8):1423-1431.

16. Harris GA, Galhena AS, Fernandez FM. Ambient sampling/ionization mass spectrometry: Applications and current trends. *Anal Chem (Washington, DC, U S)*. 2011;83(12):4508-4538.

17. Venter A, Sojka PE, Cooks RG. Droplet dynamics and ionization mechanisms in desorption electrospray ionization mass spectrometry. *Anal Chem*. 2006;78(24):8549-8555.

18. Kebarle P, Verkerk UH. Electrospray: From ions in solution to ions in the gas phase, what we know now. *Mass Spectrom Rev*. 2009;28(6):898-917.

19. Kebarle P. A brief overview of the present status of the mechanisms involved in electrospray mass spectrometry. *J Mass Spectrom*. 2000;35(7):804-817.

20. Nefliu M, Smith JN, Venter A, Cooks RG. Internal energy distributions in desorption electrospray ionization (DESI). *J Am Soc Mass Spectrom*. 2008;19(3):420-427.

21. Haddad R, Milagre HMS, Catharino RR, Eberlin MN. Easy ambient sonic-spray ionization mass spectrometry combined with thin-layer chromatography. *Anal Chem (Washington, DC, U S)*. 2008;80(8):2744-2750.

22. Hirabayashi A, Sakairi M, Koizumi H. Sonic spray mass spectrometry. *Anal Chem*. 1995;67(17):2878-82.

23. Takada Y, Sakairi M, Koizumi H. Atmospheric pressure chemical ionization interface for capillary electrophoresis/mass spectrometry. *Anal Chem*. 1995;67(8):1474-1476.

24. Wiseman JM, Ifa DR, Venter A, Cooks RG. Ambient molecular imaging by desorption electrospray ionization mass spectrometry. *Nat Protocols*. 2008;3(3):517-524.

25. Takats Z, Wiseman JM, Cooks RG. Ambient mass spectrometry using desorption electrospray ionization (DESI): Instrumentation, mechanisms and applications in forensics, chemistry, and biology. *J Mass Spectrom*. 2005;40(10):1261-1275.

26. Kertesz V, Van Berkel GJ. Improved imaging resolution in desorption electrospray ionization mass spectrometry. *Rapid Commun Mass Spectrom*. 2008;22(17):2639-2644.

27. Green FM, Salter TL, Gilmore IS, Stokes P, O'Connor G. The effect of electrospray solvent composition on desorption electrospray ionisation (DESI) efficiency and spatial resolution. *Analyst.* 2010;135(4):731-7.

28. Eberlin LS, Ferreira CR, Dill AL, Ifa DR, Cheng L, Cooks RG. Nondestructive, histologically compatible tissue imaging by desorption electrospray ionization mass spectrometry. *ChemBioChem*. 2011;12(14):2129-2132.

29. Dill AL, Ifa DR, Manicke NE, et al. Lipid profiles of canine invasive transitional cell carcinoma of the urinary bladder and adjacent normal tissue by desorption electrospray ionization imaging mass spectrometry. *Anal Chem (Washington, DC, U S)*. 2009;81(21):8758-8764.

30. Wiseman JM, Ifa DR, Song Q, Cooks RG. Tissue imaging at atmospheric pressure using desorption electrospray ionization (DESI) mass spectrometry. *Angew Chem , Int Ed*. 2006;45(43):7188-7192.

31. Girod M, Shi Y, Cheng J, Cooks RG. Mapping lipid alterations in traumatically injured rat spinal cord by desorption electrospray ionization imaging mass spectrometry. *Anal Chem*. 2011;83(1):207-215.

32. Eberlin LS, Dill AL, Costa AB, et al. Cholesterol sulfate imaging in human prostate cancer tissue by desorption electrospray ionization mass spectrometry. *Anal Chem (Washington, DC, U S)*. 2010;82(9):3430-3434.

33. Ellis SR, Wu C, Deeley JM, et al. Imaging of human lens lipids by desorption electrospray ionization mass spectrometry. *J Am Soc Mass Spectrom*. 2010;21(12):2095-2104.

34. Manicke NE, Nefliu M, Wu C, et al. Imaging of lipids in atheroma by desorption electrospray ionization mass spectrometry. *Anal Chem (Washington, DC, U S)*. 2009;81(21):8702-8707.

35. Dill AL, Eberlin LS, Zheng C, et al. Multivariate statistical differentiation of renal cell carcinomas based on lipidomic analysis by ambient ionization imaging mass spectrometry. *Anal Bioanal Chem*. 2010;398(7-8):2969-2978.

36. Dill AL, Eberlin LS, Costa AB, et al. Multivariate statistical identification of human bladder carcinomas using ambient ionization imaging mass spectrometry. *Chem --Eur J*. 2011;17(10):2897-2902, S2897/1-S2897/7.

37. Eberlin LS, Dill AL, Golby AJ, et al. Discrimination of human astrocytoma subtypes by lipid analysis using desorption electrospray ionization imaging mass spectrometry. *Angew Chem , Int Ed*. 2010;49(34):5953-5956, S5953/1-S5953/12.

38. Wu C, Ifa DR, Manicke NE, Cooks RG. Molecular imaging of adrenal gland by desorption electrospray ionization mass spectrometry. *Analyst (Cambridge, U K)*. 2010;135(1):28-32.

39. Dill AL, Ifa DR, Manicke NE, et al. Lipid profiles of canine invasive transitional cell carcinoma of the urinary bladder and adjacent normal tissue by desorption electrospray ionization imaging mass spectrometry. *Anal Chem (Washington, DC, U S)*. 2009;81(21):8758-8764.

40. Wisemen JM, Ifa DR, Zhu Y, et al. Desorption electrospray ionization mass spectrometry: Imaging drugs and metabolites in tissues. *Proc Natl Acad Sci U S A*. 2008;105(47):18120-18125, S18120/1-S18120/9.

41. Watrous J, Hendricks N, Meehan M, Dorrestein PC. Capturing bacterial metabolic exchange using thin film desorption electrospray ionization-imaging mass spectrometry. *Anal Chem (Washington, DC, U S)*. 2010;82(5):1598-1600.

42. Muller T, Oradu S, Ifa DR, Cooks RG, Krautler B. Direct plant tissue analysis and imprint imaging by desorption electrospray ionization mass spectrometry. *Anal Chem*. 2011;83(14):5754-61.

43. Li B, Bjarnholt N, Hansen SH, Janfelt C. Characterization of barley leaf tissue using direct and indirect desorption electrospray ionization imaging mass spectrometry. *J Mass Spectrom*. 2011;46(12):1241-1246.

44. Lalli PM, Sanvido GB, Garcia JS, et al. Fingerprinting and aging of ink by easy ambient sonic-spray ionization mass spectrometry. *Analyst (Cambridge, U K)*. 2010;135(4):745-750.

45. Saraiva SA, Abdelnur PV, Catharino RR, Nunes G, Eberlin MN. Fabric softeners: Nearly instantaneous characterization and quality control of cationic surfactants by easy ambient sonic-spray ionization mass spectrometry. *Rapid Commun Mass Spectrom*. 2009;23(3):357-362.

46. Eberlin LS, Haddad R, Sarabia Neto RC, et al. Instantaneous chemical profiles of banknotes by ambient mass spectrometry. *Analyst (Cambridge, U K)*. 2010;135(10):2533-2539.

47. Alberici RM, Simas RC, de Souza V, de Sa GF, Daroda RJ, Eberlin MN. Analysis of fuels via easy ambient sonic-spray ionization mass spectrometry. *Anal Chim Acta*. 2010;659(1-2):15-22.

48. Cooks RG, Ouyang Z, Takats Z, Wiseman JM. Ambient mass spectrometry. *Science (Washington, DC, U S)*. 2006;311(5767):1566-1570.

49. Watrous, J. D.; Dorrestein, P. C. Imaging mass spectrometry in microbiology. ***NatureReviews Microbiology*** **2011, *9*, 683-694.**

50. Hamid TS, Lostun D, Cabral EC, Garrett R, Bohme DK, Ifa DR. Comparisons of ambient spray ionization imaging methods. ***Int J Mass Spectrom*****. 2014:Ahead of Print.**

51. Janfelt C, Norgaard AW. Ambient mass spectrometry imaging: A comparison of desorption ionization by sonic spray and electrospray. ***J Am Soc Mass Spectrom*****. 2012;23(10):1670-1678.**

52. Zhang Y, Yuan Z, Dewald HD, Chen H. Coupling of liquid chromatography with mass spectrometry by desorption electrospray ionization (DESI). ***Chemical Communications*****. 2011;47(14):4171-4173.**

53. Takats Z, Wiseman JM, Cooks RG. Ambient mass spectrometry using desorption electrospray ionization (DESI): Instrumentation, mechanisms and applications in forensics, chemistry, and biology. ***J Mass Spectrom*****. 2005;40(10):1261-1275.**

54. Hu Q, Talaty N, Noll RJ, Cooks RG. Desorption electrospray ionization using an orbitrap mass spectrometer: Exact mass measurements on drugs and peptides. ***Rapid Communications in Mass Spectrometry*****. 2006;20(22):3403-3408.**

55. Haddad R, Sparrapan R, Kotiaho T, Eberlin MN. Easy ambient sonic-spray ionization-membrane interface mass spectrometry for direct analysis of solution constituents. ***Anal Chem*****. 2008;80(3):898-903.**

56. Haddad R, Sparrapan R, Eberlin MN. Desorption sonic spray ionization for (high) voltage-free ambient mass spectrometry. ***Rapid Communications in Mass Spectrometry*****. 2006;20(19):2901-2905.**

57. Eberlin LS, Ifa DR, Wu C, Cooks RG. Three-dimensional vizualization of mouse brain by lipid analysis using ambient ionization mass spectrometry. ***Angewandte Chemie-International Edition*****. 2010;49(5):873-876.**

58. Chramow A, Hamid TS, Eberlin LS, Girod M, Ifa DR. Imaging of whole zebra fish (danio rerio) by desorption electrospray ionization mass spectrometry. ***Rapid Commun Mass Spectrom*****. 2014;28(19):2084-2088.**

59. Love DR, Pichler FB, Dodd A, Copp BR, Greenwood DR. Technology for high-throughput screens: The present and future using zebrafish. ***Curr Opin Biotechnol*****. 2004;15(6):564-571.**

60. Stern H, Zon L. Opinion - cancer genetics and drug discovery in the zebrafish. ***Nature Reviews Cancer*****. 2003;3(7):533-539.**

61. Cowart LA. Sphingolipids: Players in the pathology of metabolic disease. *Trends in Endocrinology and Metabolism*. 2009;20(1):34-42.

62. Wiseman JM, Ifa DR, Song Q, Cooks RG. Tissue imaging at atmospheric pressure using desorption electrospray ionization (DESI) mass spectrometry. *Angew Chem , Int Ed*. 2006;45(43):7188-7192.

63. Reschly EJ, Ai N, Ekins S, et al. Evolution of the bile salt nuclear receptor FXR in vertebrates. *J Lipid Res*. 2008;49(7):1577-1587.

64. Nelson KA, Daniels GJ, Fournie JW, Hemmer MJ. Optimization of whole-body zebrafish sectioning methods for mass spectrometry imaging. *J Biomol Tech*. 2013;24(3):119-27.

65. Jackson SN, Wang HJ, Woods AS. In situ structural characterization of glycerophospholipids and sulfatides in brain tissue using MALDI-MS/MS. *J Am Soc Mass Spectrom*. 2007;18(1):17-26.

66. Eberlin LS, Liu X, Ferreira CR, Santagata S, Agar NYR, Cooks RG. Desorption electrospray ionization then MALDI mass spectrometry imaging of lipid and protein distributions in single tissue sections. *Anal Chem*. 2011;83(22):8366-8371.

67. Eberlin LS, Norton I, Dill AL, et al. Classifying human brain tumors by lipid imaging with mass spectrometry. *Cancer Res*. 2012;72(3):645-654.

68. Hsu FF, Bohrer A, Turk J. Electrospray ionization tandem mass spectrometric analysis of sulfatide. determination of fragmentation patterns and characterization of molecular species expressed in brain and in pancreatic islets. *Biochimica Et Biophysica Acta-Lipids and Lipid Metabolism*. 1998;1392(2-3):202-216.

69. Plhalova L, Stepanova S, Praskova E, et al. The effects of subchronic exposure to metribuzin on danio rerio. *Scientific World Journal*. 2012:728189.

70. Li Q, Chen S, Zhang S, et al. Bioconcentration study of xinjunan in zebrafish. *Environ Monit Assess*. 2011;183(1-4):113-120.

71. Jonsson CM, Toledo MCF. Acute toxicity of endosulfan to the fish hyphessobrycon bifasciatus and brachydanio rerio. *Arch Environ Contam Toxicol*. 1993;24(2):151.

72. Kates, M. Techniques of Lipidology. Science. 1986; 1: 464.

73. Siegel GJ et al. Basic Neurochemistry: Molecular, Cellular and Medical Aspects, 1999, 6th Ed.

74. Shin Y, Drolet B, Mayer R, Dolence K, Basile F. Desorption electrospray ionization-mass spectrometry of proteins. *Anal Chem*. 2007;79(9):3514-3518.

75. Douglass KA, Venter AR. Protein analysis by desorption electrospray ionization mass spectrometry and related methods. *Journal of Mass Spectrometry*. 2013;48(5):553-560.

76. Takats Z, Wiseman JM, Cooks RG. Ambient mass spectrometry using desorption electrospray ionization (DESI): Instrumentation, mechanisms and applications in forensics, chemistry, and biology. *Journal of Mass Spectrometry*. 2005;40(10):1261-1275.

77. Inutan ED, Wager-Miller J, Mackie K, Trimpin S. Laserspray ionization imaging of multiply charged ions using a commercial vacuum MALDI ion source. *Anal Chem*. 2012;84(21):9079-9084.

78. Kaltashov IA, Mohimen A. Estimates of protein surface areas in solution by electrospray ionization mass spectrometry. *Anal Chem*. 2005;77(16):5370-5379.

79. Miao Z, Wu S, Chen H. The study of protein conformation in solution via direct sampling by desorption electrospray ionization mass spectrometry. *J Am Soc Mass Spectrom*. 2010;21(10):1730-1736.

80. Chen Y, Mori M, Pastusek AC, Schug KA, Dasgupta PK. On-line electrodialytic salt removal in electrospray ionization mass spectrometry of proteins. *Anal Chem*. 2011;83(3):1015-1021.

81. Winger B, Lightwahl K, Loo R, Udseth H, Smith R. Observation and implications of high mass-to-charge ratio ions from electrospray-ionization mass-spectrometry. *J Am Soc Mass Spectrom*. 1993;4(7):536-545.

Appendix A: List of abbreviations:

ABBREVIATION	DESCRIPTION
MeOH	Methanol
ACN	Acetonitrile
DMF	Dimethylformamide
PE	Phosphatidylethanolamine